NORTHWESTERN UNIVERSITY

On Initiation of Polymerization Waves in Thermal Free-Radical Frontal Polymerization

A DISSERTATION

SUBMITTED TO THE GRADUATE SCHOOL

IN PARTIAL FULFILLMENT OF THE REQUIREMENTS

for the degree of

DOCTOR OF PHILOSOPHY

Field of Applied Mathematics

By

Laura Rylie Ritter

EVANSTON, ILLINOIS

December 2003

ABSTRACT

On Initiation of Polymerization Waves in
Thermal Free-Radical Frontal Polymerization

Laura Rylie Ritter

Thermal, frontal polymerization is a process of converting monomer into polymer via a self-propagating reaction wave. In a typical experiment, two species, a monomer and an initiator, are placed in a test tube, and the temperature at one end is increased by applying a heat source. The temperature increase induces decomposition of initiator into active radicals allowing polymer chain growth to begin. The exothermic chemical conversion occurs in a narrow reaction zone, and the heat released by the reaction induces further decomposition of initiator just ahead of the front. In this way, a self-sustained reaction wave can travel through the mixture. Insufficient input of heat, inadequate amounts of reactants, and volumetric heat loss are some factors that can inhibit reaction front formation (initiation).

We consider thermal frontal polymerization processes given different experimental conditions. First, we consider a system with a prescribed heat influx as the heat source supplied. Using large activation energy asymptotics, we track the temperature from the inert to the transition heating stages. The initiation criterion is derived as a two parameter integral equation. Depending on the parameter values, the solution to the integral equation exhibits blow-up behavior indicating initiation or remains bounded indicating noninitiation. Next, we replace the heat flux with a fixed temperature at the end of the tube and allow for Newtonian heat loss. We numerically derive an initiation criterion as a function of initiator consumption, volumetric heat loss, the initial mixture temperature, and the adiabatic increase in

temperature . Finally, we examine the phenomenon of spontaneous front formation in the center of a tube of monomer and initiator immersed in a hot bath. Heat supplied by the bath raises the temperature of the mixture allowing for a reaction front to form; however, if a reaction does begin, the temperature of the front is much larger than the bath which then serves as a heat sink. Through a numerical examination we confirm that front formation at the center of the mixture can occur. Because of the dual effects of the oil bath, front formation depends on the relationship between bath temperature and tube radius.

To my parents John and Janet Ritter

In loving memory of Rylie Ritter, Mercedes Sharp, and Tieko the bird

Acknowledgments

First, I want to thank my advisors Ed Olmstead and Volodia Volpert for their efforts and the patience they always showed when working with me. Volodia never failed to make time for me and showed incredible tolerance for even the silliest of my questions. His extensive knowledge of applied mathematics and his ability to explain difficult concepts has been invaluable to my work here. I hope to develop my mathematical and teaching skills by his most excellent example. I want to thank Ed Olmstead for agreeing to work with me at a time when he was not considering taking any students. This work could not even have begun without his mathematical insights and his willingness to share them with me. I greatly appreciate the trust he showed in me when he allowed me to teach for him and develop my skills as an instructor. And, I am grateful to him for bringing me into the family of past students he has worked with as these contacts will help me to build my future in academia.

I want to also thank several people who have made my time here at Northwestern fun and rewarding. I owe a huge debt of gratitude to Judy for all of her words of support and for all of the time she took from her own personal schedule to take care of my pets. I was able to travel with confidence knowing my babies were in good hands. My office mates, Jeff, Mike, Divya, and Donna have played an invaluable

role in my experience here. I have benefited from their knowledge of applied math and polymerization. But more importantly, I have enjoyed immensely the laughter and fun we have shared. I want to thank Mike in particular: he was the first student in the department to reach out to me at the beginning of my first year, and we had many good talks about the graduate student experience from the "older student" perspective. I would like to thank Edla for her kindness and her help with little funding and other details through out my years here. I would also like to thank Michael Miksis and Alvin Bayliss for reading and commenting on this thesis and for their efforts serving on my defense committee.

To my family, I am deeply grateful. I am thankful to my parents who have believed in me through the years and have supported my educational endeavors even when I wondered if I was truly up to the task. To my sister Chandra, I owe thanks for being my best friend. Living near Chandra and spending so much time with her has been the high light of my life in Evanston. I could not have come this far without her and the rest of my family.

Finally, I must acknowledge the love of my life, my cat Tuscany. I have depended on her companionship during each stage of my work here at Northwestern. She has brightened even my most difficult days.

Contents

List of Figures

List of Tables

Chapter 1

Introduction

Thermal frontal polymerization is a process of converting a monomer into a polymer by means of a self-propagating, high temperature reaction wave. The chemical process is usually free-radical polymerization which involves two species: a monomer and an initiator which is needed to start the growth of polymer chains. In a typical experiment, the species are placed in a test tube, and the temperature at the end of the tube is increased by applying a heat source. The increase in temperature induces decomposition of the initiator which produces active radicals, and the polymer chain growth process begins. Chemical conversion then occurs in a narrow, localized region. The polymer chain growth occurring in this reaction zone is highly exothermic, and the resulting heat release promotes initiator decomposition ahead of the front. In this way a self-sustained reaction wave can form. This wave travels through the unreacted mixture leaving polymer in its wake.

Self-propagating high-temperature synthesis waves were first discovered by Merzhanov, Borovinskaya and Shkiro in 1967 in the context of combustion problems. Their experiments consisted of compressing a powdered mixture of elements into a

pellet and igniting the pellet at one end. This resulted in the formation of a reaction front which traveled through the mixture in a self-propagating mode. This process, called *self-propagating high-temperature synthesis* (SHS), was used to produce technologically useful ceramic and intermetallic materials [19]. After the initial input of heat, the reaction is driven by the energy it produces thus reducing production cost. SHS also had the advantage of producing superior quality materials. This approach to free-radical polymerization was introduced by Chechilo *et al.* in 1972 [6]. They discovered *frontal polymerization* using vinyl monomers. Chechilo *et al.* conducted several studies of the character of the polymerization process under varying experimental conditions ([3], [4], [5]). Their results were confirmed by other groups in the Soviet Union during the early 1970s, and there have since been a few other Russian studies of frontal polymerization ([9], [27], [29] [7]). Experimental studies were resumed in the United States by Pojman during the 1990s. Pojman and others observed polymerization fronts using methacrylic acid [23], undiluted liquid monomer ([24], [26]), and solid monomer [25]. In frontal polymerization, the production of polymer is both rapid and uniform. Continued study of the phenomenon is motivated by the expected benefits over traditional polymerization techniques: namely lower energy cost, reduced waste production, and increased control of product features and quality [12].

Khanukaev *et al.* first conducted theoretical examinations of the process of frontal polymerization in 1974 ([13], [14], [15]), and later Goldfeder *et al.* , and Spade and Volpert, studied a mathematical model for a five species reaction. In [8] and [28], this model is presented, and traveling wave solutions are sought. In these theoretical examinations of the process, the focus has been on the propagation of the thermal front and its velocity, the spatial profiles of the species involved, the degree

of conversion of monomer, and the final temperature of the mixture. Initiation of a polymerization front is presumed. From experimental work, however, it is found that initiation of the front does not always occur. The dependence of initiation on the amount of reactants at the onset of the experiment, the initial temperature, the heat control imposed at the end of the test tube, and the properties of the initiator is desired.

The purpose of this dissertation is to examine the initiation process necessary for propagation. In this respect, the current study is similar to ignition considerations in solid phase combustion problems. Unlike the combustion problem with a single reactant, the frontal polymerization process involves several chemical reaction steps with different reaction rates and activation energies. However, the reaction mechanism in both processes is assumed to be Arrhenius, and upon nondimensionalization of the kinetic equations governing frontal polymerization we can obtain a system of partial differential equations of a similar form as those arising in solid phase combustion. For this reason, the techniques applied in the first part of the current analysis are similar to those that have been used to study ignition of a combustible half space. In particular, we use a high activation energy asymptotic analysis to study the equations governing the system. In this way, we show that the mechanism governing initiation of the polymerization front gives rise to a two parameter integral equation governing the temperature in the transitional heating stage. The integral equation derived here is new to the field of frontal polymerization as well as the study of combustible solids. However, this integral equation appears as an extension to similar integral equations that are known in condensed phase combustion studies. In the special case that reactant consumption is negligible, the integral equation derived in this study reduces to an integral equation first introduced by

Liñàn and Williams (1971) in the study of a combustible solid exposed to a constant influx of heat [17]. This was again derived by Kapila (1981) under the assumption of uniform energy input [11] and later by Olmstead (1983) who considered an arbitrary influx of heat with heat loss by convection allowed at the end of the solid [21]. In 1987, Lasseigne and Olmstead studied ignition of a combustible half-space and accounted for reactant consumption. In [16], they derived a one parameter integral equation governing ignition. The integral equation in [16] can also be recovered from the integral equation derived in the current work by considering a limiting case.

An asymptotic and numerical analysis of the integral equation shows that two qualitatively different types of solutions exist. Depending on the parameter values the equation has solutions that blow-up in finite time or solutions that are global. These two types of behavior are interpreted as indicating initiation and non-initiation of a polymerization front, respectively. Moreover, we can determine the critical parameter values that separate the initiation and non-initiation regimes. This resulting initiation criterion is then studied in terms of its dependence on the physical and chemical properties of any particular mixture (e.g. initial amounts of reactants, activation energies, pre-exponential factors etc.), as well as the energy flux imposed during the experiment.

In chapter 2 of this work, we give a mathematical formulation of the frontal polymerization process. We begin with the chemical kinetics and derive a system of differential equations describing the state of an experimental mixture. The focus is then narrowed to the particular phenomenon of initiation of polymerization waves, and the relevant equations are given. In chapter 3, the system of equations is analyzed asymptotically, and an initiation criterion is derived in the form of an integral equation as discussed. A thorough analysis of the integral equation is the

focus of chapter 4. Here, we will address existence considerations as well as the types of solutions to the integral equation that do exist. The integral equation is then solved numerically for various parameter values and an account of these results is presented. A discussion of the problem considered and concluding remarks are included in chapter 4. In the final chapter, we consider the question of whether initiation occurs under different experimental setups. The primary tool of analysis used in this chapter is numerical. In the first part of chapter 5, we examine the same problem considered in chapters 2–4 but for a different imposed heat source and now allowing for heat losses to the environment. An initiation criterion is sought in terms of the relationship between various parameters inherent to the process. In the final part of chapter 5, a numerical analysis of a phenomenon reported by Asakura *et al.* in [1] is presented. Asakura and co-workers observed spontaneous formation of a polymerization front at the center of a cylindrical tube and subsequent propagation radially outward toward the tube walls. This occurred as the mixture was placed in a hot isothermal bath, but the front formation (or lack thereof) appeared to depend on the bath temperature and the radius of the tube. A model of this is introduced in §5.2, and numerical results are presented. We find that initiation of a polymerization front is seen to occur or fail to occur based on test tube radius for any fixed bath temperature.

Chapter 2

A Mathematical Formulation of Initiation of Polymerization Waves Given a Prescribed Heat Flux

In [20], a chemical model of radical chain polymerization is given. The process is identified by a sequence of three events, *initiation*, *propagation*, and *termination* which are carried out in five chemical reactions. We consider a typical experiment of free-radical frontal polymerization in which a mixture of monomer and initiator are placed into a test tube and a heat source is imposed at one end of the tube. The first event, initiation, is induced as the initiator is thermally unstable. This consists of two chemical reactions : 1. The initiator decomposes to produce free radicals (decomposition), and 2. A free radical combines with a monomer molecule to produce a polymer radical (chain initiation). Letting I, R, and M represent the initiator, primary free radicals, and the monomer respectively, and $\dot{P}_i$ represent a polymer radical consisting of i monomer molecules, the chemical reactions are given

by

$$I \xrightarrow{k_d} f \times 2R$$

$$R + M \xrightarrow{k_i} \dot{P}_1$$
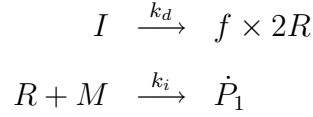
The term f appearing in the decomposition equation is the efficiency factor which is the ratio of free radicals that are consumed by monomer molecules to the total free radicals formed by the initiator. Typically, $f \approx 1/2$ [8].

Once the polymer chain is initiated, the propagation step is carried out by the successive addition of monomer molecules to the active polymer chain. Hundreds or thousands of monomer molecules may be added in this fashion, and after each addition the polymer chain is identical except larger by a single monomer unit [20]. The chemical reaction for this propagation step can be expressed as

$$\dot{P}_i + M \xrightarrow{k_p} \dot{P}_{i+1}$$
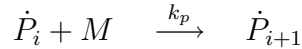
for $i = 1, 2, 3, \ldots$.

Finally, the polymerization is completed by termination when the polymer radical combines with a free radical (primary radical termination) or with another polymer radical (polymer radical termination). The two chemical equations

$$R + \dot{P}_n \xrightarrow{k_e} P$$

$$\dot{P}_n + \dot{P}_m \xrightarrow{k_t} P \tag{2.1}$$

describe this termination step. Here, P denotes the final polymer product.

In each of these equations, the reaction rates, denoted by k with a subscript, are assumed to have an Arrhenius dependence on the temperature of the system. Thus, they can be expressed as

$$k_* = k_*^0 \exp\left(\frac{-E_*}{R_g T}\right).$$

Here, k_*^0 is the pre-exponential factor, E_* is the activation energy for the corresponding reaction, R_g is the universal gas constant, T is the temperature of the mixture, and $* = d, i, p, e$ or t according to the reaction step. The values of k_*^0 and E_* are assumed to be constants; their values are determined by the choice of monomer and initiator. The temperature T is a function of position in the mixture as well as time. It is governed by a reaction diffusion equation as will be described.

2.1 Mathematical Model

For our mathematical formulation of the problem, we will assume that the radius of the test tube used for the experiment is small relative to its length. Then, we can model the tube as a one-dimensional semi-infinite region $\hat{x} \geq 0$. A mathematical model for the five species reaction described above is derived in [8] and [28]. The following system of equations governing the kinetics at time $\hat{t}$ in dimensional coordinates is given:

$$\frac{dI}{d\hat{t}} = -k_d I \tag{2.2}$$

$$\frac{dR}{d\hat{t}} = 2fk_d I - k_i RM - k_e R\dot{P} \tag{2.3}$$

$$\frac{dM}{d\hat{t}} = -k_i RM - k_p M\dot{P} \tag{2.4}$$

$$\frac{d\dot{P}}{d\hat{t}} = k_i RM - k_e R\dot{P} - 2k_t \dot{P}^2 \tag{2.5}$$

$$\frac{dP}{d\hat{t}} = k_e R\dot{P} + k_t \dot{P}^2 \tag{2.6}$$

The concentration of each of the five species is given in mol/L, and the notation for the polymer radicals contains an implied summation ($\dot{P} = \Sigma_n \dot{P}_n$).

In addition to the evolution of the species, we consider the energy balance in the system. To that end, we note that the decomposition step is slightly endothermic but that each of the four subsequent reactions is exothermic. Each of these four reactions therefore contributes to the net enthalpy of the system. However, it has been determined that the most significant heat release occurs in the propagation step [18] . Only this contribution to the net energy of the system will be considered here. Let $T(\hat{t}, \hat{x})$ denote the temperature of the mixture at time $\hat{t}$ and at the point $\hat{x}$ along the tube, and let $\kappa > 0$ (assumed constant) be the thermal diffusivity of the mixture. We define the parameter $q = -\Delta H/(c\rho)$ as the increase in temperature induced per unit reacted monomer. The quantity (assumed constant) ΔH is the heat of the propagation reaction, and the constants c and ρ are the specific heat and density of the mixture, respectively. We can write the following reaction diffusion equation governing the temperature:

$$\frac{\partial T}{\partial \hat{t}} = \kappa \frac{\partial^2 T}{\partial \hat{x}^2} - q \frac{\partial M}{\partial \hat{t}}. \tag{2.7}$$

Equations (2.2)–(2.7), together with appropriate initial and boundary conditions, completely describe the state of the mixture. Because the current study is concerned with initiation of a polymerization front, we will consider a reduced system obtained by imposing the quasi-steady-state assumption (QSSA) [28], reducing the number of unknowns as in [8] and [28], and considering only the evolution of the initiator, the monomer, and the temperature. The QSSA states that the level of primary and polymer radicals in the mixture is nearly constant. Hence, we put $(d/d\hat{t})(R + \dot{P}) = 0$.

In addition, we make the simplifying assumptions as justified in [28]

$$k_i = k_p, \quad k_e = k_t, \quad \text{and} \quad \dot{P} \gg R.$$

We can add equations (2.3) and (2.5). Then, making the aforementioned assumptions we arrive at the algebraic equation for R and $\dot{P}$

$$R + \dot{P} \approx \sqrt{\frac{2fk_d}{k_t}}\sqrt{I}.$$

Upon substitution of the above into equation (2.4), the evolution of the monomer can be written as

$$\frac{dM}{d\hat{t}} = -k_p\sqrt{\frac{2fk_d}{k_t}}M\sqrt{I}.$$

Noting that the coefficient in front of M in the above equation is an Arrhenius exponential motivates the following convenient notation for the effective reaction rate:

$$k_{eff} = k_p\sqrt{\frac{2fk_d}{k_t}}, \quad k_{eff}^0 = k_p^0\sqrt{\frac{2fk_d^0}{k_t^0}}, \quad \text{and} \quad E_{eff} = \frac{1}{2}(E_d - E_t) + E_p.$$

The initial amounts of monomer and initiator present are known and will be denoted by M_0 and I_0. Similarly, the initial temperature of the system is given as T_0. We will begin by assuming that the boundary condition on the temperature at $\hat{x} = 0$ will be a Neumann condition. That is, the heat flux is prescribed as

$$\frac{\partial T}{\partial \hat{x}} = -\hat{h}(\hat{t}), \quad \text{for} \quad \hat{x} = 0, \, \hat{t} > 0.$$

Further, we assume that $\hat{h}(\hat{t}) > 0$ for all $\hat{t}$. This restriction implies an energy input at the end of the test tube. Finally, the temperature far from the reaction is assumed

to be equal to the initial temperature. The reduced, dimensional form of the system to be studied can then be written as

$$\frac{\partial I}{\partial \hat{t}} = -k_d(T)I, \quad I(0) = I_0 \tag{2.8}$$

$$\frac{\partial M}{\partial \hat{t}} = -k_{eff}(T)M\sqrt{I}, \quad M(0) = M_0 \tag{2.9}$$

$$\frac{\partial T}{\partial \hat{t}} = \kappa \frac{\partial^2 T}{\partial \hat{x}^2} + qk_{eff}(T)M\sqrt{I}, \quad T(0, \hat{x}) = T_0 \quad \hat{x} \geq 0, \tag{2.10}$$

$$\frac{\partial T(\hat{t}, 0)}{\partial \hat{x}} = -\hat{h}(\hat{t}), \quad \text{and} \quad T \to T_0 \quad \text{as} \quad x \to \infty. \tag{2.11}$$

The asymptotic analysis is based on the scaling of various parameters governing the above system. In the following section, a nondimensionalization of equations (2.8)–(2.11) is given, and the scaling assumptions are discussed.

2.2   Scaling and Nondimensionalization

We derive an initiation criterion through large activation energy asymptotics. Because the activation energies in the frontal polymerization process are relatively large, the Arrhenius reaction terms are insignificant at the onset of the experiment when the temperature is relatively small. This motivates a scaling of the temperature by some critical temperature T_c at which the reaction term first becomes appreciable. A clarification of this constant is needed, and this issue will be addressed later. Further, the largeness of the activation energies facilitates a perturbation

scheme in solving for the temperature. Hence, we introduce the small parameter

$$\epsilon = R_g T_c / E_{eff}.$$

We can nondimensionalize equations (2.8)–(2.11) by defining the quantities

$$r = \frac{E_d}{E_{eff}}, \qquad \tilde{k}_d^0 = k_d^0 e^{-r/\epsilon}, \quad \tilde{k}_{eff}^0 = k_{eff}^0 e^{-1/\epsilon},$$

$$t_* = (\tilde{k}_{eff}^0 \sqrt{I_0})^{-1}, \qquad \text{and} \qquad x_* = \sqrt{\kappa t_*}.$$

We also introduce the nondimensional variables

$$\phi = I/I_0, \qquad \psi = M/M_0, \quad \theta = T/T_c, \quad \theta_0 = T_0/T_c,$$

$$h(t) = \frac{x_*}{T_c} \hat{h}(\hat{t}), \quad t = \hat{t}/t_*, \qquad \text{and} \qquad x = \hat{x}/x_*.$$

From equations (2.8)–(2.11) and the above definitions, we obtain the corresponding nondimensional system:

$$\frac{\partial \phi}{\partial t} = -A\phi \exp\left\{ \frac{r}{\epsilon}\left(1 - \frac{1}{\theta}\right) \right\}, \quad \phi(0) = 1 \tag{2.12}$$

$$\frac{\partial \psi}{\partial t} = -\psi\sqrt{\phi}\exp\left\{ \frac{1}{\epsilon}\left(1 - \frac{1}{\theta}\right) \right\}, \quad \psi(0) = 1 \tag{2.13}$$

$$\frac{\partial \theta}{\partial t} = \frac{\partial^2 \theta}{\partial x^2} + B\psi\sqrt{\phi}\exp\left\{ \frac{1}{\epsilon}\left(1 - \frac{1}{\theta}\right) \right\}, \quad \theta(0, x) = \theta_0 \tag{2.14}$$

$$\frac{\partial \theta(t, 0)}{\partial x} = -h(t), \quad \text{and} \quad \theta \to \theta_0 \quad \text{as} \quad x \to \infty. \tag{2.15}$$

The additional nondimensional parameters A and B appearing in equations (2.12) and (2.14) are defined by

$$A = \frac{\tilde{k}_d^0}{\tilde{k}_{eff}^0 \sqrt{I_0}}, \quad \text{and} \quad B = \frac{M_0 q}{T_c}.$$

The potential for initiation of polymerization waves is inherent in the scaling of these two parameters; A is a measure of the rate of consumption of initiator, and B is a measure of how exothermic chain propagation is. If A is large, for example, we can expect that the amount of initiator will rapidly decay. This rapid decay or an insufficient quantity of initiator at the onset of the experiment will cause the reaction to stop before a thermal front can develop. Similarly, if B is small, the effect of the reaction term in (2.14) is decreased. This can result in insufficient heat to initiate and maintain propagation of the polymer chain. In the present analysis, the following scaling will be assumed:

$$A = A_0 \epsilon^{-1} \quad \text{and} \quad B = B_0 \epsilon^{-\frac{1}{2}}$$

with $A_0 = O(1)$ and $B_0 = O(1)$ with respect to ϵ. The numerical values of A, B, and ϵ depend on the choice of reactants, their kinetic properties, and the conditions of the experiment (e.g. pressure and ambient temperature). Extensive tabulated values of activation energies, pre-exponential factors, and other kinetic parameters for various initiators and monomers can be found in [2]. For typical values of the physical parameters appearing in equations (2.8)–(2.11), the value of ϵ is expected to be in the range of 10^{-4} to 10^{-3}. Moreover, at room temperature the values of A_0 and B_0 can range between 0.01 to 10. Given the typical range of values for ϵ,

this is consistent with the assumption that A_0 and B_0 are $O(1)$ with respect to ϵ. The critical temperature T_c used in the scaling is defined implicitly by the expression

$$A = \frac{k_d(T_c)}{k_{eff}(T_c)\sqrt{I_0}} \qquad (2.16)$$

for any fixed value of A_0.

The appearance of the parameter r present in the exponent of equation (2.12) is a characteristic that distinguishes this system from the similar equations appearing in solid phase combustions studies. Typical activation energies associated with frontal polymerization are such that $E_d \gg E_p \gg E_t$. Hence this parameter, the ratio of decomposition activation energy to the effective propagation activation energy, is such that $1 < r \leq 2$. Equations (2.12)–(2.15) and the parameters discussed complete our formulation of the problem.

Chapter 3

The Initiation Criterion

In this chapter, we find that the initiation process is described by a two parameter integral equation. The system under consideration, (2.12)–(2.15), is restated here for convenience:

$$\frac{\partial \phi}{\partial t} = -A\phi \exp\left\{\frac{r}{\epsilon}\left(1 - \frac{1}{\theta}\right)\right\}, \quad \phi(0) = 1$$

$$\frac{\partial \psi}{\partial t} = -\psi\sqrt{\phi}\exp\left\{\frac{1}{\epsilon}\left(1 - \frac{1}{\theta}\right)\right\}, \quad \psi(0) = 1$$

$$\frac{\partial \theta}{\partial t} = \frac{\partial^2 \theta}{\partial x^2} + B\psi\sqrt{\phi}\exp\left\{\frac{1}{\epsilon}\left(1 - \frac{1}{\theta}\right)\right\}, \quad \theta(0, x) = \theta_0$$

$$\frac{\partial \theta(t, 0)}{\partial x} = -h(t), \quad \text{and} \quad \theta \to \theta_0 \quad \text{as} \quad x \to \infty.$$

Here, the parameter $\epsilon \ll 1$, A and B are of the order ϵ^{-1} and $\epsilon^{-1/2}$ respectively, and $1 < r \le 2$.

3.1 Inert Heating

As stated, we consider the initial temperature to be small so that the reaction terms are negligible at the onset of the experiment—during the inert heating stage. In the formulation above, this means that we take $\theta_0 < 1$ and $1 - \theta_0 = O(1)$ with respect to ϵ. This allows us to initially ignore the Arrhenius term, which is mathematically equivalent to taking the limit $\epsilon \to 0$ in (2.12)–(2.14). Let θ_I be given by

$$\theta_I(t, x) = \theta_0 + \int_0^t h(\tau) \frac{e^{\frac{-x^2}{4(t-\tau)}}}{\sqrt{\pi(t - \tau)}} \, d\tau. \tag{3.1}$$

Then θ_I solves the problem (2.14)–(2.15) in the limit $\epsilon \to 0$; θ_I is the so-called inert heating solution. From $0 < 1 - \theta_0$ and $1 - \theta_0 = O(1)$, it follows that initially

$$\theta = \theta_I + \text{e.s.t.}$$

where e.s.t. represents terms that are exponentially small with respect to ϵ. This approximation, however, only remains valid until such time as $\theta_I \approx 1$. In order to continue the analysis, let us define the critical time t_c to be the smallest value such that

$$1 = \theta_I(t_c, 0) = \theta_0 + \int_0^{t_c} \frac{h(\tau)}{\sqrt{\pi(t_c - \tau)}} \, d\tau.$$

For arbitrary $h(t)$, such a critical time need not exist. This suggests a restriction on the class of boundary conditions that can lead to initiation. We will assume that

the imposed flux $h(t)$ given is such that this critical time does exist. Also note that the above is evaluated at $x = 0$ because θ_I attains its maximum at the end $x = 0$. The inert stage of the reaction ends in the neighborhood of $(t_c, 0)$. At this point, the system enters a transition heating stage where the reaction terms are no longer negligible.

To further our investigation, we perturb about $(t_c, 0)$ and introduce the new independent variables

$$\xi = x/\epsilon, \quad \tau = (t - t_c)/\epsilon.$$

In these inner variables and with the assumed scaling for A and B, equations (2.12)–(2.15) can be written as

$$\phi_\tau = -A_0 \phi \exp\left\{ \frac{r}{\epsilon} \left(1 - \frac{1}{\theta} \right) \right\}, \quad \phi \to 1 \quad \text{as} \quad \tau \to -\infty \tag{3.2}$$

$$\psi_\tau = -\epsilon \psi \sqrt{\phi} \exp\left\{ \frac{1}{\epsilon} \left(1 - \frac{1}{\theta} \right) \right\}, \quad \psi \to 1 \quad \text{as} \quad \tau \to -\infty \tag{3.3}$$

$$\epsilon \theta_\tau = \theta_{\xi\xi} + \epsilon^{3/2} B_0 \psi \sqrt{\phi} \exp\left\{ \frac{1}{\epsilon} \left(1 - \frac{1}{\theta} \right) \right\}, \quad \theta \to \theta_0 \quad \text{as} \quad \tau \to -\infty \tag{3.4}$$

$$\theta_\xi = O(\epsilon) \quad \text{for} \quad \xi = 0 \quad \text{and} \quad \tau > -\infty. \tag{3.5}$$

We note here that the conditions at $t = 0$ in the outer variables corresponds asymptotically to conditions in the inner variables as $\tau \to -\infty$. Also, we see that equations (3.2) and (3.3) can be integrated to determine ϕ and ψ in terms of θ.

That is,

$$\phi(\tau) \;=\; \exp\left(-A_0 \int_{-\infty}^{\tau} e^{\frac{r}{\epsilon}\left(1-\frac{1}{\theta}\right)} \, ds\right) \tag{3.6}$$

$$\psi(\tau) \;=\; \exp\left(-\epsilon \int_{-\infty}^{\tau} e^{\frac{1}{\epsilon}\left(1-\frac{1}{\theta}\right)} \times e^{-\frac{A_0}{2}\int_{-\infty}^{s} e^{\frac{r}{\epsilon}\left(1-\frac{1}{\theta}\right)} \, dq} \, ds\right). \tag{3.7}$$

Substitution of these results into (3.4)–(3.5) yields a single problem in the dependent variable θ.

3.2 Transition Stage Heating

3.2.1 An Asymptotic Expansion

We seek an asymptotic expansion for θ of the form

$$\theta = \theta_I + \epsilon\theta^0 + \epsilon^{3/2}\theta^1 + \dots$$

Then, we can expand θ_I about $(t_c, 0)$ and write

$$\theta_I = 1 + \epsilon a\tau - \epsilon b\xi + o(\epsilon) \tag{3.8}$$

where

$$a = \lim_{t \to t_c} \frac{\partial \theta_I}{\partial t}, \quad \text{and} \quad b = -\lim_{x \to 0} \frac{\partial \theta_I}{\partial x}.$$

For the continued analysis, we must assume that these limits exist and that $a > 0$ and $b > 0$. The latter condition follows from requiring that h is a non-negative function for all time corresponding to an influx of energy at the end of

the test tube. The condition $a > 0$ implies that the temperature be increasing at the onset of the transition phase. Both of these conditions are consistent with the potential for initiation.

Substitution of (3.8) into the expansion of θ yields

$$\theta = 1 + \epsilon(a\tau - b\xi + \theta^0) + \epsilon^{3/2}\theta^1 + o(\epsilon^{3/2})$$

so that

$$\frac{1}{\epsilon}\left(1 - \frac{1}{\theta}\right) = (a\tau - b\xi + \theta^0) + o(1).$$

Combining this result with (3.6) and (3.7), and substituting into the boundary value problem (3.4)–(3.5), we arrive at the equations governing θ^0 and θ^1:

$$\theta^0_{\xi\xi} = 0$$

$$O(\epsilon):$$

$$\theta^0(-\infty, \xi) = 0, \quad \theta^0_\xi(\tau, 0) = 0, \tag{3.9}$$

$$\theta^1_{\xi\xi} = -B_0 e^{a\tau - b\xi + \theta^0} \exp\left(\frac{-A_0}{2} \int_{-\infty}^\tau e^{r(as - b\xi + \theta_0)} \, ds\right)$$

$$O(\epsilon^{3/2}): \tag{3.10}$$

$$\theta^1(-\infty, \xi) = 0, \quad \theta^1_\xi(\tau, 0) = 0.$$

Equation (3.9) has solution

$$\theta^0(\tau, \xi) = f_0(\tau), \quad \text{where} \quad f_0(\tau) \to 0 \text{ as } \tau \to -\infty.$$

This is substituted into (3.10) to obtain

$$\theta^1(\tau, \xi) = -B_0 e^{a\tau + f_0(\tau)} \int_0^\xi \int_0^z e^{-b\hat{z}} \exp\left(\frac{-A_0}{2} e^{-rb\hat{z}} \int_{-\infty}^\tau e^{r(as + f_0(s))} \, ds \right) d\hat{z} \, dz + f_1(\tau),$$

with $f_1(\tau) \to 0$ as $\tau \to -\infty$.

The temperature in the transition heating stage is governed by the nature of the leading correction $f_0(\tau)$.

3.2.2   Matching to the Outer Solution

In order to determine the leading correction f_0, we need a matching condition for large ξ. To this end, we consider the stretched space variable

$$X = \sqrt{\epsilon}\xi.$$

Let $\hat{\Theta}$ represent the solution in the boundary layer. From equation (3.4), we have

$$\hat{\Theta}_\tau = \hat{\Theta}_{XX} + O(\epsilon^{1/2}).$$

Assuming θ has the following form in the boundary layer

$$\theta = \theta_I + \epsilon\hat{\Theta}^0 + \epsilon^{3/2}\hat{\Theta}^1 + \dots$$

the $O(\epsilon)$ problem is

$$\hat{\Theta}_\tau^0 = \hat{\Theta}_{XX}^0, \quad \hat{\Theta}^0 \to 0 \text{ as } \tau \to -\infty. \tag{3.11}$$

Additional conditions at $X = 0$ are needed and are determined by matching to the outer solution. Observe that as $X \to 0$ and $\xi \to \infty$,

$$\epsilon \hat{\Theta}^0 + \epsilon^{3/2} \hat{\Theta}^1 + \ldots \quad = \quad \epsilon \theta^0 + \epsilon^{3/2} \theta^1 + \ldots \tag{3.12}$$

$$\epsilon \hat{\Theta}^0_X + \epsilon^{3/2} \hat{\Theta}^1_X + \ldots \quad = \quad 0 + \epsilon^{3/2} \theta^1_X + \ldots$$

$$= \quad 0 + \epsilon^{3/2} (\epsilon^{-1/2} \theta^1_\xi) + \ldots \tag{3.13}$$

Equating by powers in ϵ, the above implies that

$$\lim_{X \to 0} \hat{\Theta}^0(\tau, X) \quad = \quad \lim_{\xi \to \infty} \theta^0(\tau, \xi) \tag{3.14}$$

and

$$\lim_{X \to 0} \hat{\Theta}^0_X(\tau, X) \quad = \quad \lim_{\xi \to \infty} \theta^1_\xi(\tau, \xi). \tag{3.15}$$

From equation (3.11) and the conditions (3.14) and (3.15), we see that Θ^0 is governed by

$$\hat{\Theta}^0_\tau \quad = \quad \hat{\Theta}^0_{XX}$$

$$\hat{\Theta}^0_X(\tau, 0) \quad = \quad -B_0 e^{a\tau + f_0(\tau)} \int_0^\infty e^{-bz} e^{\frac{-A_0}{2} e^{-rbz} \int_{-\infty}^\tau e^{r(as + f_0(s))} \, ds} \, dz \tag{3.16}$$

$$\equiv \quad \Lambda(\tau)$$

$$\hat{\Theta}^0 \to 0 \quad \text{as} \quad \tau \to -\infty.$$

The additional condition

$$\hat{\Theta}^0(\tau, 0) = f_0(\tau)$$

determines the unknown function f_0. The solution of (3.16) can be expressed in terms of the Green's function

$$\hat{\Theta}^0(X, \tau) = - \int_{-\infty}^{\tau} \Lambda(\sigma) G(X, \tau; 0, \sigma) \, d\sigma,$$

where

$$G(X, \tau; 0, \sigma) = \frac{1}{\sqrt{\pi(\tau - \sigma)}} e^{\frac{-X^2}{4(\tau - \sigma)}}.$$

Finally, applying the condition on $\hat{\Theta}^0$ at $X = 0$, we arrive at the nonlinear integral equation governing the temperature in the transition stage:

$$f_0(\tau) = - \int_{-\infty}^{\tau} \frac{\Lambda(\sigma)}{\sqrt{\pi(\tau - \sigma)}} \, d\sigma = \frac{B_0}{b} \int_{-\infty}^{\tau} \frac{e^{f_0(\sigma) + a\sigma}}{\sqrt{\pi(\tau - \sigma)}} Q(\sigma) \, d\sigma, \qquad (3.17)$$

where

$$Q(\sigma) = \int_0^{\infty} b e^{-bz} \exp\left(-e^{-rbz} \frac{A_0}{2} \int_{-\infty}^{\sigma} e^{r(f_0(s) + as)} \, ds \right) \, dz.$$

In the next chapter, we will examine the integral equation (3.17). We note here that the exponential in the integrand is monotonically increasing in f_0, while the term Q is decreasing in f_0. We will see that these represent the competing effects of the heat release from polymerization propagation which promotes front formation and the consumption of reactants which serves to inhibit this formation. We will perform a coordinate change resulting in the appearance of a parameter governing the qualitative behavior of the solution. Existence considerations will be addressed, and both analytical and numerical results presented.

Chapter 4

The Integral Equation

Recall that the parameter r was defined as the ratio of the decomposition activation energy to the effective activation energy obtained by applying the QSSA. Typical experimental values of the activation energy for decomposition, propagation and termination are such that $E_d \gg E_p \gg E_t$. From the definition of the effective activation energy and r,

$$E_{eff} = \frac{1}{2}(E_d - E_t) + E_p \quad \text{and} \quad r = \frac{E_d}{E_{eff}},$$

it follows that the ratio r is roughly 2. We will consider only values of r such that $1 < r \leq 2$ with special attention given to the case $r = 2$. The integral Q appearing in (3.17) can be expressed in terms of gamma functions. Note that

$$
\begin{aligned}
Q(\sigma) &= \int_0^\infty b e^{-bz} \exp\left(-e^{-rbz}\frac{A_0}{2}\int_{-\infty}^{\sigma} e^{r(f_0(s)+as)}\,ds\right)\,dz \\
&= \frac{\Gamma\left(\frac{1}{r}\right)}{r}\,\gamma\left(\frac{1}{r}, q(\sigma)\right),
\end{aligned}
$$

where

$$q(\sigma) = \frac{A_0}{2} \int_{-\infty}^{\sigma} e^{r(f_0(s)+as)} \, ds,$$

Γ is the gamma function, and γ is the incomplete gamma function defined by

$$\gamma(\alpha, z) = \frac{z^{-\alpha}}{\Gamma(\alpha)} \int_0^z e^{-t} t^{\alpha-1} \, dt.$$

To facilitate the analysis of the integral equation, let us introduce the change of variables

$$\eta = a\tau + \log\left(\frac{B_0}{b\sqrt{a}}\right) \quad \text{and} \quad u(\eta) = f_0(\tau).$$

In these new coordinates, (3.17) takes the form

$$u(\eta) = \int_{-\infty}^{\eta} \frac{e^{u(\sigma)+\sigma}}{\sqrt{\pi(\eta-\sigma)}} F_r\left(\lambda_r \int_{-\infty}^{\sigma} e^{r(u(s)+s)} \, ds\right) d\sigma. \tag{4.1}$$

The function F_r appearing above is defined by

$$F_r(x) = \frac{\Gamma\left(\frac{1}{r}\right)}{r} \gamma\left(\frac{1}{r}, x\right) \quad \text{for} \quad x > 0, \quad \text{with} \quad F_r(0) = 1,$$

and the parameter λ_r is the ratio

$$\lambda_r = a^{r/2-1} \frac{A_0 b^r}{2 B_0^r} \geq 0.$$

Note that in the case $r = 2$,

$$F_2(x) = \frac{\sqrt{\pi}}{2} \frac{\text{erf}(\sqrt{x})}{\sqrt{x}},$$

and

$$\lambda_2 = \frac{A_0 b^2}{2B_0^2}.$$

A number of observations should be made about the parameter λ_r and the function F_r defined above. First, in the limiting case, $\lambda_r = 0$ ($F_r \equiv 1$), equation (4.1) reduces to the integral equation derived by Liñàn and Williams [17], Kapila [11], and Olmstead [21] governing the ignition of a combustible half space with negligible reactant consumption. It is known that this equation has a solution u that is positive, monotonically increasing. Moreover, this solution exhibits an infinite singularity in finite time. The following asymptotic behavior of u has been determined for this case

$$u \sim e^\eta + \frac{1}{\sqrt{2}} e^{2\eta} + \ldots \quad \text{as} \quad \eta \to -\infty$$

$$u \sim -\frac{1}{2} \log(\eta^* - \eta) + \ldots \quad \text{as} \quad \eta \to \eta^*$$

with $\eta^* \approx -0.431$ the numerically determined "blow-up time".

Also, for every value of r, F_r is positive, monotonically decreasing, with $F_r \to 0$ as its argument tends to infinity. If $r = 1$, then equation (4.1) is exactly that obtained by Lasseigne and Olmstead [16] governing ignition of a solid half space with first order Arrhenius reaction and accounting for reactant consumption. They found that there is a critical value of the parameter λ_1 such that for values less than this critical value the solution u becomes unbounded in finite time—it is this unbounded behavior that is taken to signal the onset of ignition. For values of λ_1 larger than this critical value, the solution remains bounded for all finite time. Large λ_r values can be thought of as indicating a weakly exothermic reaction or a mixture with

insufficient reactants, while small λ_r values indicate a highly exothermic reaction with adequate reactants and sufficient heat release.

The decaying nature of F_r serves to inhibit initiation of a polymerization front. This is the case for all r on $1 < r \leq 2$. However, for fixed x note that $(d/dr) F_r(x) > 0$. Hence, as r increases, F_r decays less rapidly. As will be shown in §4.3, $r = 2$ appears to be an upper limit for the possible existence of solutions exhibiting the type of logarithmic singularity analogous to those discussed in [21] and [16].

4.1 Existence of solutions to the integral equation

We continue the analysis by establishing the existence of solutions to (4.1). Through these existence considerations, we will establish a lower bound on the possible initiation time. The analysis also reveals a relationship between this lower bound and the parameter λ_r. We begin by considering the set of uniformly bounded functions

$$S = \{u : (-\infty, \tilde{\eta}] \to [0, N]\}$$

where $\tilde{\eta} > -\infty$ and $0 < N < \infty$. And, let the integral operator T be given by

$$Tu \longmapsto \int_{-\infty}^{\eta} \frac{e^{u(\sigma)+\sigma}}{\sqrt{\pi(\eta - \sigma)}} F_r \left(\lambda_r \int_{-\infty}^{\sigma} e^{r(u(s)+s)} \, ds \right) \, d\sigma, \quad \text{for} \quad \eta \leq \tilde{\eta}, \ u \in S.$$

Conditions on $\tilde{\eta}$ and N are sought to ensure that T is a contraction on S.

For $u \in S$ observe that

$$\frac{1}{r} e^{r\sigma} \leq \int_{-\infty}^{\sigma} \exp(rs + ru(s)) \, ds \leq \frac{1}{r} e^{rN+r\sigma} \quad \text{for} \quad -\infty < \sigma \leq \tilde{\eta}. \qquad (4.2)$$

Since F_r is decreasing this implies that

$$F_r\left(\frac{\lambda_r}{r}e^{rN+r\sigma}\right) \leq F_r\left(\lambda_r \int_{-\infty}^{\sigma} \exp(rs + ru(s))\, ds\right) \leq F_r\left(\frac{\lambda_r}{r}e^{r\sigma}\right).$$

It follows that,

$$Tu \leq e^N I_0(\eta; r, \lambda_r),$$

where

$$I_0(\eta; r, \lambda_r) = \int_{-\infty}^{\eta} \frac{e^\sigma}{\sqrt{\pi(\eta - \sigma)}} F_r\left(\frac{\lambda_r}{r}e^{r\sigma}\right) d\sigma.$$

We see that T maps S into S provided

$$I_0(\eta; r, \lambda_r) \leq Ne^{-N}.$$

Second, let u_1 and u_2 be elements of S. For ease of notation let

$$I(u, \sigma) = \int_{-\infty}^{\sigma} \exp(rs + ru(s))\, ds.$$

Then note that

$$|Tu_1 - Tu_2| \leq \int_{-\infty}^{\eta} \frac{e^\sigma}{\sqrt{\eta - \sigma}} \left|e^{u_1} F_r(\lambda_r I(u_1, \sigma)) - e^{u_2} F_r(\lambda_r I(u_2, \sigma))\right| d\sigma$$

$$\leq \sup_{u_1, u_2 \in S} |u_1 - u_2| \int_{-\infty}^{\eta} \frac{e^\sigma}{\sqrt{\eta - \sigma}} \left|\frac{e^{u_1} F_r(\lambda_r I(u_1, \sigma)) - e^{u_2} F_r(\lambda_r I(u_2, \sigma))}{u_1 - u_2}\right| d\sigma$$

$$\leq \sup_{u_1,u_2 \in S} |u_1 - u_2| \int_{-\infty}^{\eta} \frac{e^{\sigma}}{\sqrt{\eta - \sigma}} \left\{ \sup_{u^* \in S} \left| \frac{d}{du} e^{u^*} F_r(\lambda I(u^*, \sigma)) \right| \right\} d\sigma$$

$$\leq \sup_{u_1,u_2 \in S} |u_1 - u_2| e^N \int_{-\infty}^{\eta} \frac{e^{\sigma}}{\sqrt{\eta - \sigma}} \left\{ F_r \left(\frac{\lambda_r}{r} e^{r\sigma} \right) + W \right\} d\sigma$$

where

$$W = \lambda_r \sup_{u^* \in S} |F_r'(\lambda I(u^*, \sigma))| \frac{d}{du} I(u^*, \sigma),$$

u^* is some element of S between u_1 and u_2, and $F_r'(x)$ denotes the derivative of F_r with respect to x. Since $|F_r'(x)|$ is monotonically decreasing in x and using the relation (4.2), we have that

$$|F_r'(\lambda I(u^*, \sigma))| \leq \left| F_r' \left(\frac{\lambda_r}{r} e^{r\sigma} \right) \right|$$

for all $u^* \in S$. Then

$$|Tu_1 - Tu_2| \leq \sup_{u_1,u_2 \in S} |u_1 - u_2| \left\{ e^N I_0(\eta; r, \lambda_r) + e^{(r+1)N} I_1(\eta; r, \lambda_r) \right\},$$

where

$$I_1(\eta; r, \lambda_r) = \lambda_r \int_{-\infty}^{\eta} \frac{e^{(r+1)\sigma}}{\sqrt{\pi(\eta - \sigma)}} \left| F_r' \left(\frac{\lambda_r}{r} e^{r\sigma} \right) \right| d\sigma.$$

Since I_0 and I_1 are monotonically increasing in η (see appendix A), we can conclude that T is a contraction on S provided

$$I_0(\tilde{\eta}; r, \lambda_r) \leq N e^{-N} \tag{4.3}$$

and

$$e^N I_0(\tilde{\eta}; r, \lambda_r) + e^{(r+1)N} I_1(\tilde{\eta}; r, \lambda_r) < 1. \tag{4.4}$$

For given $\lambda_r > 0$, there exists a unique pair $\hat{N} < 1$, $\hat{\eta} > -\infty$ such that (4.3) and (4.4) are satisfied as equalities (see appendix B). That is,

$$e^{\hat{N}} I_0(\hat{\eta}; r, \lambda_r) = \hat{N}$$

$$e^{\hat{N}} I_0(\hat{\eta}; r, \lambda_r) + e^{(r+1)\hat{N}} I_1(\hat{\eta}; r, \lambda_r) = 1.$$

Inequalities (4.3) and (4.4) are satisfied for $N = \hat{N}$ and any choice of $\tilde{\eta} < \hat{\eta}$. We note that the value of $\hat{\eta}(\lambda_r)$ provides a lower bound on the time of initiation for given λ_r. Moreover, $\hat{N}$ and $\hat{\eta}$ have the following asymptotic expansions for $\lambda_r \ll 1$ and $\lambda_r \to \infty$:

$$\hat{N} \sim 1 - \frac{\lambda_r}{(r+1)^{3/2}} + \dots$$

$$\hat{\eta} \sim -1 + \frac{\lambda_r}{r e^r (r+1)^{3/2}} + \dots \quad \text{as} \quad \lambda_r \to 0$$

and

$$\hat{N} \sim \hat{N}_\infty + \dots$$

$$\hat{\eta} \sim \lambda_r^{2/r} \left(\frac{\pi}{4 \Gamma^2(\frac{1}{r})} r^{2-2/r} \right) \hat{N}_\infty^2 e^{-2\hat{N}_\infty} + \dots \quad \text{as} \quad \lambda_r \to \infty.$$

The value $\hat{N}_\infty$ is the solution to the transcendental equation $\hat{N}_\infty = (1 - \hat{N}_\infty) e^{-r\hat{N}_\infty}$.

For $1 < r \leq 2$, the value of $\hat{N}_\infty$ is such that $0.33 \leq \hat{N}_\infty < 0.41$. Also, $1 < r \leq 2$ and $\hat{\eta} = O(\lambda_r^{2/r})$ as $\lambda_r \to \infty$ suggests that the onset of initiation can be delayed as long as desired by taking λ_r sufficiently large. Based on this finding and the known behavior of the solutions for the case $r = 1$, we anticipate two qualitatively different types of solutions to (4.1) depending on the value of λ_r. Self consistent analyses for solutions that remain bounded in finite time and those that exhibit an unbounded singularity at a finite time are sought. Such solutions are interpreted as indicating noninitiation and initiation of a front respectively. Moreover, for a given r, we seek a critical value λ_r^c separating the initiation and noninitiation regimes.

4.2 Noninitiation solutions

First, we consider the existence of solutions bounded for all finite η. To this end, assume that the solution u has the following form:

$$u \sim C\eta^d, \quad \text{as} \quad \eta \to \infty \tag{4.5}$$

where C and d are constants to be determined. If $\lambda_r > 0$ and $d < 1$, then (4.5) implies

$$e^{u+\eta} F_r\left(\lambda_r \int_{-\infty}^{\eta} e^{r(u+s)}\, ds\right) \sim \frac{\Gamma(\frac{1}{r})}{r}\left(\frac{r}{\lambda_r}\right)^{1/r} \quad \text{as} \quad \eta \to \infty.$$

For each $\eta \gg 1$, we can write

$$u(\eta) = C_0 + \Omega(\eta),$$

where Ω is defined as

$$\Omega(\eta) = \frac{1}{\sqrt{\pi}} \int_0^\eta \frac{e^{u+\eta}}{\sqrt{\eta-\sigma}} F_r \left(\lambda_r \int_{-\infty}^\sigma e^{r(u+s)}\, ds \right)\, d\sigma.$$

Employing the asymptotic techniques given in [10], we find that as $\eta \to \infty$,

$$\Omega(\eta) \sim \frac{2\Gamma(\frac{1}{r})}{r\sqrt{\pi}} \left(\frac{r}{\lambda_r} \right)^{1/r} \eta^{1/2} + \dots \tag{4.6}$$

Hence, u has the form given in (4.5) with the constants determined as

$$C = \frac{2\Gamma(\frac{1}{r})}{r\sqrt{\pi}} \left(\frac{r}{\lambda_r} \right)^{1/r} \quad \text{and} \quad d = \frac{1}{2}.$$

Note that $d < 1$ which is consistent with our initial requirement. If λ_r is large enough so as to advance the damping effect of F_r appearing in the integrand of (4.1), the leading order behavior of the solution is expected to be square root growth. In section §4.4.2, numerical confirmation of this is presented.

4.3 Initiation solutions

Next, we look for solutions of (4.1) that become unbounded at some finite time value η^*. In the case $\lambda_r = 0$, we know that the solution of (4.1) has a logarithmic singularity as previously discussed. This motivates looking for behavior of the form

$$u \sim -\beta \log(\eta^* - \eta) + \dots \quad \text{as} \quad \eta \to \eta^* \tag{4.7}$$

where $\beta = \beta(\lambda_r)$ and $\eta^* = \eta^*(\lambda_r) < \infty$. The analysis is facilitated by translating the singularity to the point at infinity. The techniques for analyzing the asymptotic behavior of certain integral equations given in [10] and [22] can then be used. In the coordinates

$$\rho = (\eta^* - \eta)^{-1} \quad v(\rho) = u(\eta),$$

equation (4.1) becomes

$$v(\rho) = \sqrt{\rho}\, e^{\eta^*} \int_0^\rho \frac{e^{v - s^{-1}}}{\sqrt{\pi(\rho - s)}} s^{-3/2} F_r \left(\lambda_r e^{r\eta^*} \int_0^s t^{-2} e^{rv - rt^{-1}}\, dt \right)\, ds, \qquad (4.8)$$

and the asymptotic behavior of v is sought as ρ tends to infinity. The cases $1 < r < 2$ and $r = 2$ must be considered separately as they give rise to different matching requirements.

Suppose $1 < r < 2$ and

$$v \sim \log(\rho^{1/2}) + \log(P) + \log(1 + o(\rho^{1/2})) \quad \text{as} \quad \rho \to \infty, \qquad (4.9)$$

where P is constant. Then, as $\rho \to \infty$

$$\frac{e^{v - 1/\rho}}{\rho^{3/2}} F_r \left(\lambda_r e^{r\eta^*} \int_0^\rho t^{-2} e^{rv - rt^{-1}}\, dt \right) \sim P\rho^{-1} F_r(\lambda_r e^{r\eta^*} I_r(\infty)) + o(\rho^{-1}),$$

where

$$I_r(\infty) = \int_0^\infty \frac{e^{rv-r/t}}{t^2} \, dt < \infty.$$

By the results in [10] and [22], it follows that

$$\int_0^\rho \frac{e^{v-1/s}}{s^{3/2}} F_r(\lambda_r e^{r\eta^*} I_r(s)) \frac{ds}{\sqrt{\pi(\rho-s)}} \sim \frac{P}{\sqrt{\pi}} F_r(\lambda_r e^{r\eta^*} I_r(\infty)) \rho^{-1/2} \log(\rho) \qquad (4.10)$$

as $\rho \to \infty$. Comparison of (4.9) and (4.10) yields

$$P = \frac{\sqrt{\pi} e^{-\eta^*}}{2 F_r(\lambda_r e^{r\eta^*} I_r(\infty))}.$$

Hence,

$$v \sim \frac{1}{2} \log(\rho) + O(1) \quad \text{as} \quad \rho \to \infty,$$

and, returning to the previous coordinates, we have

$$u \sim \frac{-1}{2} \log(\eta^* - \eta) + O(1) \quad \text{as} \quad \eta \to \eta^*.$$

We must consider a different expansion when $r = 2$. In this case, we look for the solution of (4.8) to have the asymptotic form

$$v \sim \log(\rho^\beta) + \log(1 + o(\rho^\beta)) \quad \text{as} \quad \rho \to \infty. \qquad (4.11)$$

Under the assumption (4.11), observe that the integral in the argument of F_2 appearing in equation (4.8) is not finite if $\beta = 1/2$. Matching can only occur if we restrict $\beta > 1/2$; this becomes a consistency condition on the analysis. Supposing that this is the case and that (4.11) holds, we find that

$$\frac{e^{v-\rho^{-1}}}{\rho^{3/2}} F_2\left(\lambda_2 e^{2\eta^*} \int_0^\rho \frac{e^{2v-2t^{-1}}}{t^2}\, dt\right) \sim \frac{\sqrt{\pi}}{2} e^{-\eta^*} \lambda^{-1/2} \rho^{-1} \sqrt{2\beta - 1} + o(\rho^{-1})$$

as $\rho \to \infty$. Then, employing the results in [10] and [22], we have

$$\rho^{-1/2} e^{-\eta^*} v(\rho) \sim \frac{\lambda_2^{-1/2}}{2} e^{-\eta^*} \sqrt{2\beta - 1} \rho^{-1/2} \log(\rho) \quad \text{as} \quad \rho \to \infty. \tag{4.12}$$

Comparing the left and right sides of this relation and using (4.11), we arrive at the equation for β:

$$\beta(\lambda_2) = \frac{1}{4\lambda_2}\left(1 - \sqrt{1 - 4\lambda_2}\right). \tag{4.13}$$

The following observations should be made about this result. First, note that $\beta > 1/2$ as was required for the derivation. Also, we see that this result can only be valid—insofar as β is real—for values of λ_2 between 0 and 0.25. This seems to suggest an upper bound of 0.25 on the critical value of λ_2. In fact, the numerical analysis confirms this where we find that $\lambda_2^c = 0.11998$. Finally, we note that $\beta \to 1/2$ as $\lambda_2 \to 0$, which is consistent with the results for $r < 2$ and those in [17] and [21] for the $\lambda_r = 0$ case. In terms of the variables u and η, the asymptotic results for the initiation case are summarized:

$$u \sim -\frac{1}{2} \log(\eta^* - \eta) + \ldots \text{ as } \quad \eta \to \eta^*(\lambda_r)$$

for $1 < r < 2$, and

$$u(\eta) \sim -\beta(\lambda_2) \log(\eta^*(\lambda_2) - \eta) + \ldots \quad \text{as} \quad \eta \to \eta^*(\lambda_2)$$

for $r = 2$ with β given by (4.13). In both cases, the value of the time at which initiation occurs η^* is to be determined numerically.

4.4   Numerical analysis

4.4.1   Numerical Methods

Equation (4.1) was solved numerically for several values of r and λ_r. Because the lower bound of the integral is infinite, the asymptotic form of the solution u as $\eta \to -\infty$ is useful. Using the properties of the incomplete gamma function and the identity

$$\int_{-\infty}^{\eta} \frac{e^{\alpha\sigma}}{\sqrt{\pi(\eta - \sigma)}} \, d\sigma = \frac{e^{\alpha\eta}}{\sqrt{\alpha}}, \quad \text{for all} \quad \alpha > 0,$$

we have

$$u \sim e^{\eta} + \frac{1}{\sqrt{2}} e^{2\eta} + \ldots \quad \text{as} \quad \eta \to -\infty, \tag{4.14}$$

and

$$\int_{-\infty}^{\sigma} e^{r(u+s)}\, ds \sim \frac{1}{r}e^{r\sigma} + \frac{r}{r+1}e^{(r+1)\sigma} + \ldots \quad \text{as} \quad \sigma \to -\infty. \tag{4.15}$$

We then fix $\eta_0 > -\infty$ and assume that for all $\eta, \sigma < \eta_0$ the relations (4.14) and (4.15) hold as equalities. Substituting (4.14) and (4.15) into (4.1) we arrive at the following equation that is solved numerically (see appendix C).

$$u(\eta) = e^{\eta}\mathrm{erfc}\sqrt{\eta - \eta_0} + \frac{1}{\sqrt{2}}e^{2\eta}\mathrm{erfc}\sqrt{2(\eta - \eta_0)}$$

$$+ \int_{\eta_0}^{\eta} \frac{e^{u+\sigma}}{\sqrt{\pi(\eta - \sigma)}} F_r\left(\lambda_r I_r(\sigma)\right)\, d\sigma,$$

where

$$I_r(\sigma) = \frac{1}{r}e^{r\eta_0} + \frac{r}{r+1}e^{(r+1)\eta_0} + \int_{\eta_0}^{\sigma} e^{r(u+s)}\, ds.$$

This approach is similar to that applied by Lasseigne and Olmstead [16]. Moreover, if $r = 1$, the above reduces to the integral equation considered in [16] for a first order reaction term. The accuracy of the numerical methods employed in the current work was tested by comparing the results obtained for $r = 1$ with those in [16]. The value $\eta_0 = -10$ was found to be sufficient to produce reliable results, and this was used for all numerical computations presented here.

4.4.2 Numerical Results

For convenience, we restate the definition of the parameter λ_r here

$$\lambda_r = a^{r/2-1}\frac{A_0 b^r}{2B_0^r},$$

and recall that A_0 and B_0 are measures of the consumption rate of initiator and heat release due to conversion of monomer, respectively; r $(1 < r \leq 2)$ is the ratio of activation energies associated with decomposition of initiator and polymer chain propagation. Thus

$$\lambda_r \propto \frac{\text{Rate of Initiator Consumption}}{\text{Heat Released by Reaction}}$$

We see that λ_r is small provided A_0 is relatively small and B_0 relatively large. Hence, we can consider small values of λ_r to represent a sufficiently exothermic reaction in which the consumption rate of initiator is small relative to the amount of initiator present in the mixture. Conversely, large values of λ_r indicate an inadequate amount of initiator (i.e. initiator is consumed to rapidly) or that heat release is insufficient to sustain further reaction. Small λ_r values are therefore expected to lead to initiation, while large values of λ_r are not. The appearance of a and b in the ratio is the effect of the inert heating, and the values of these parameters are controlled by the choice of heat source applied. As suggested by the results in [16] and the self consistent analyses in §4.2 and §4.3 of the current paper, there exists a critical value of λ_r separating the initiation and noninitiation regimes.

Table 4.1: The critical parameter value, λ_r^c, as a function of r

r	1.5	1.8	1.9	2
λ_r^c	0.6645	0.31086	0.21058	0.11998

The critical value of the parameter λ_r^c was determined numerically for different r values. The results are given in table 4.1. If $\lambda_r < \lambda_r^c$, then the solution exhibits a
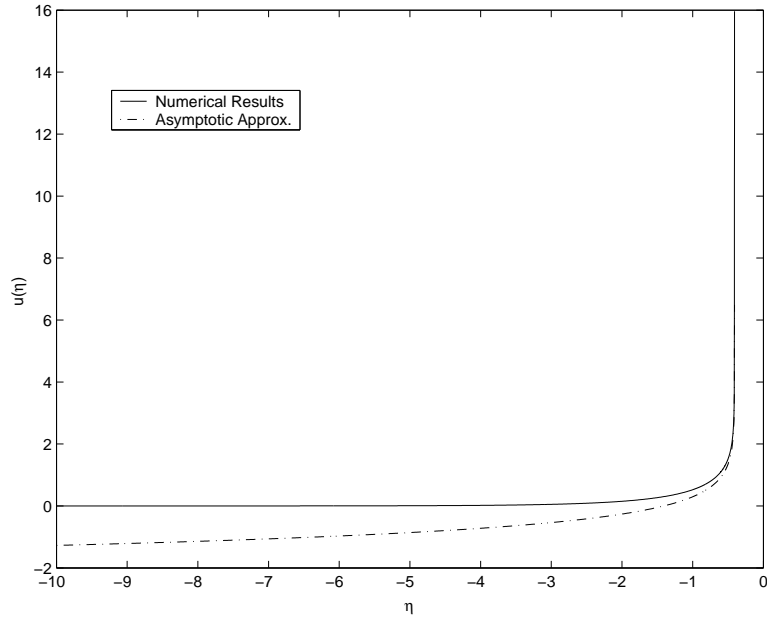
Figure 4.1: Initiation solution of the integral equation for $r = 2$ and $\lambda_2 = 0.1$ The solution approaches the asymptotic approximation $U = -\beta(0.1)\log(\eta^* - \eta)$ as $\eta \to \eta^* \approx -0.4088$.

logarithmic singularity with the asymptotic behavior described in §4.3. For values of λ_r larger than λ_r^c, the solution to (4.1) exists and is finite for all η. When λ_r is only slightly larger than the critical value, the solution exhibits behavior on two time scales (see figure 4.3). The temperature grows slowly while oscillating on a short time scale. This results from the competing effects of the exponential term appearing in (4.1) and the decaying function F_r. If λ_r is increased further, the solution has the leading form described in §4.2

Table 4.2: Initiation time η^* for selected values of λ_2

λ_2	0	0.01	0.1	0.117	0.11997
η^*	-0.4310	-0.4287	-0.4088	-0.4048	-0.4037
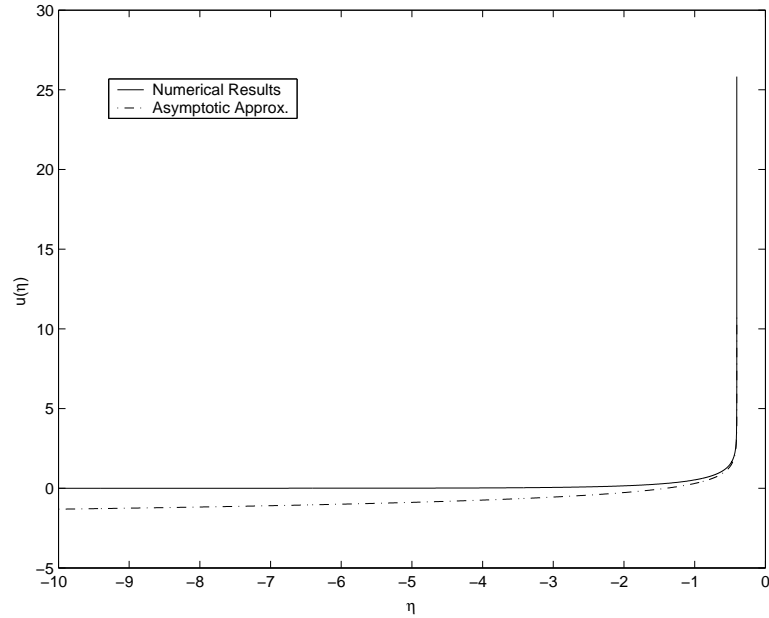
Figure 4.2: Initiation solution of the integral equation for $r = 2$ and $\lambda_2 = 0.11997$—just below the critical value of 0.11998. The solution approaches the asymptotic approximation $U = -\beta(0.11997)\log(\eta^* - \eta)$ as $\eta \to \eta^* \approx -0.4037$.

The time at which initiation occurs for the case $r = 2$ is given in table 4.2 for various λ_2 with the critical value found to be 0.11998. Solutions of the types described above for $r = 2$ are shown in figures 4.1–4.4. In figure 4.1, λ_2 is less than the critical value. The solution becomes unbounded at $\eta = -0.4088$. The asymptotic results are shown as a dashed curve for comparison. Similarly, figure 4.2 shows the initiation solution for $\lambda_2 = 0.11997$, just slightly less than the critical value. In both cases, the singular behavior indicates that the temperature progresses beyond the transition stage and a polymerization front is formed. In contrast, figures 4.3 and 4.4 show the solution when λ_2 is above the critical value. In figure 4.3, $\lambda_2 = 0.4$ and the temperature oscillations described can be seen. However, the large scale behavior is slow growth with the oscillations damping as η increases. Figure

4.4 is a plot of the solution when $\lambda_2 = 1$. Here, the solution is monotonic with a change of concavity occurring in a neighborhood of $\eta = 0$. The temperature remains bounded indicating that a reaction front does not form.
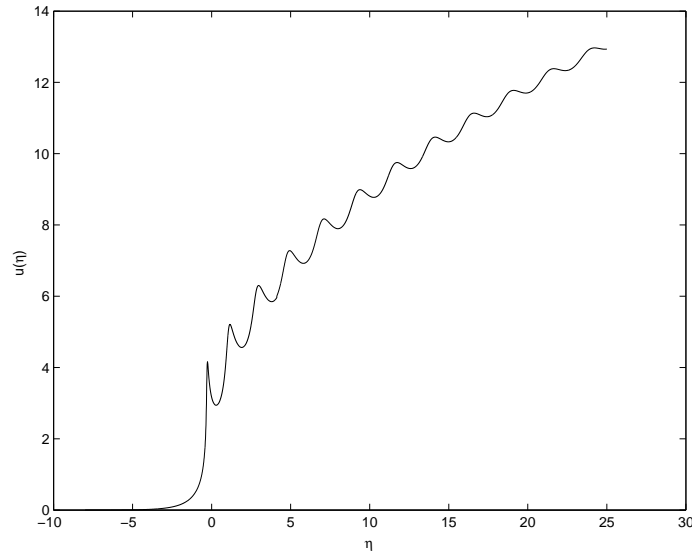
Figure 4.3: The noninitiation solution showing oscillation for $r = 2$ and $\lambda_2 = 0.4$

4.4.3 Discussion

A reduced system governing a five species reaction model of free-radical frontal polymerization was considered, and the temperature was tracked from the inert heating to the transition stage. Through an asymptotic analysis, the integral equation (3.17) arose as the first correction to the inert solution. This integral equation was then rewritten by a change of variables as equation (4.1) where there appears the parameter λ_r which governs the qualitative behavior of the solution. For a fixed ratio of the activation energies, there is a critical value of the parameter λ_r^c such that the solution of (4.1) has an infinite singularity in finite time if $\lambda_r < \lambda_r^c$ but
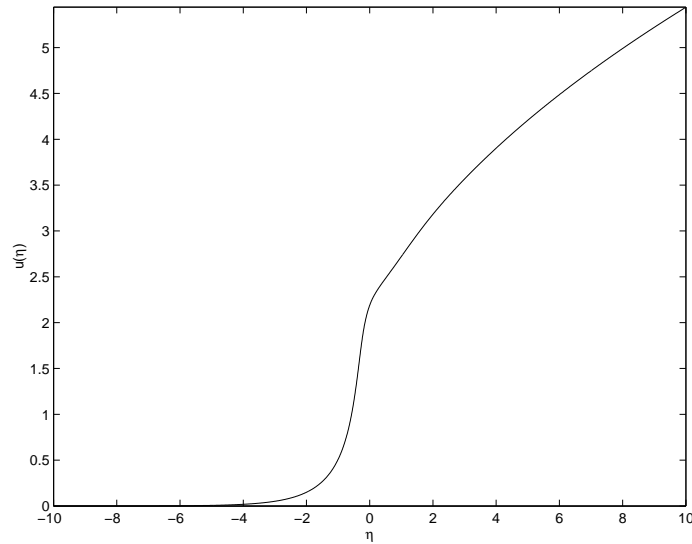
Figure 4.4: The noninitiation solution for $r = 2$ and $\lambda_2 = 1$

remains bounded for all time if $\lambda_r > \lambda_r^c$.

The unbounded and bounded types of solutions are taken to indicate initiation and noninitiation in the underlying system. Initiation being the formation and onset of propagation of a polymerization front. In the noninitiation case, but for values of λ_r close to the critical value, an oscillatory type of solution was found numerically. The solution remains bounded in this case, and it appears that the oscillations dampen with the growth of the independent variable.

The experimental parameters can be chosen so as to ensure the onset of a thermal front. The critical temperature T_c used in the scaling can be determined by fixing A_0 in the relation (2.16). This results in a transcendental equation for T_c

$$A_0 \frac{E_{eff}}{R_g T_c} = \frac{k_d(T_c)}{k_{eff}(T_c)\sqrt{I_0}}.$$

Then, B_0 can be found in terms of the initial amount of monomer and the heat release parameter q, and the values a and b are given in terms of the known flux

condition.

As an example, we consider the case of constant heat flux $h(t) = \theta_e$ prescribed at the end of the tube ($x = 0$). The inert heating solution can be found explicitly from (3.1)

$$\theta_I(t,x) = \theta_0 + \theta_e\left(2\sqrt{\frac{t}{\pi}}e^{-\frac{x^2}{4t}} - x\operatorname{erfc}\left(\frac{x}{2\sqrt{t}}\right)\right).$$

The values of t_c (satisfying $\theta_I(t_c,0) = 1$), a, and b are then determined from the above in terms of θ_0 and θ_e. Fixing A_0 and considering T_c as a varying parameter, we can obtain a marginal initiation criterion for the initial amount of initiator I_0 and the initial temperature T_0 (in dimensional quantities). For a given r the two relations

$$\lambda_r^c = a^{r/2-1}\frac{A_0 b^r}{2B_0}$$

$$A_0 = \frac{R_g T_c}{E_{eff}}\frac{k_d(T_c)}{k_{eff}(T_c)}I_0^{-1/2} = \text{constant}$$

define the parametric equations $I_0(T_c)$ and $T_0(T_c)$. In figures 4.5 and 4.6, plots of I_0 and T_0 are presented for $A_0 = 0.1$ and the parameter values as given in the accompanying tables. An increase in the initial temperature means an increased amount of initiator needs to be present in the mixture to ensure formation and propagation of a reaction wave. This is the case because increasing T_c results in an increase in the rate of consumption of initiator and is indicative of a reduced influx of heat at the end of the tube ($\theta_e \propto T_c^{-1}$). Figures 4.5a and 4.6a indicate the minimum initial amount of initiator necessary to induce initiation of a reaction wave for any fixed value of the initial temperature.

Some additional comments regarding the relationship of the integral equation (4.1) to the original system (2.12)–(2.15) and the limitations of the results are in order. First, we have shown that under certain conditions, the solution to the integral equation (4.1) exhibits an infinite singularity at a finite time. This singular behavior is interpreted as thermal runaway and hence initiation of a polymerization front. This does not, however, correspond to blow-up of the solution of the original system (2.12)–(2.15) of interest in this study. For the system, (2.12)–(2.15), there exists a unique, global solution as indicated by the classical theory of parabolic equations. However, the Arrhenius reaction term produces a large temperature gradient at the site of initiation so that the temperature profile at the end of the tube exhibits a steep increase to the maximum temperature in a thin reaction zone. It is this sharp increase in temperature that is modeled asymptotically by the thermal runaway phenomenon of the integral equation (4.1).

Second, we note that even in the case that thermal runaway occurs in equation (4.1)—i.e. the parameter values are such that $\lambda_r < \lambda_r^c$—the front formed requires a sufficiently large amount of initiator present in the mixture for propagation throughout the tube. While it is possible to induce runaway by imposing a sufficiently high level of external energy input at $x = 0$, this case is not of interest since the reaction will die off and the polymer will not be produced. Hence, for the results obtained here to be of practical use, the values of a and b must be assumed to be $O(1)$ and fixed as prescribed by the externally imposed heat flux. Then, the variation in the magnitude of λ_r can be viewed as due to changes in the values of A_0 and B_0 which correspond to the physical and chemical properties of any particular mixture.
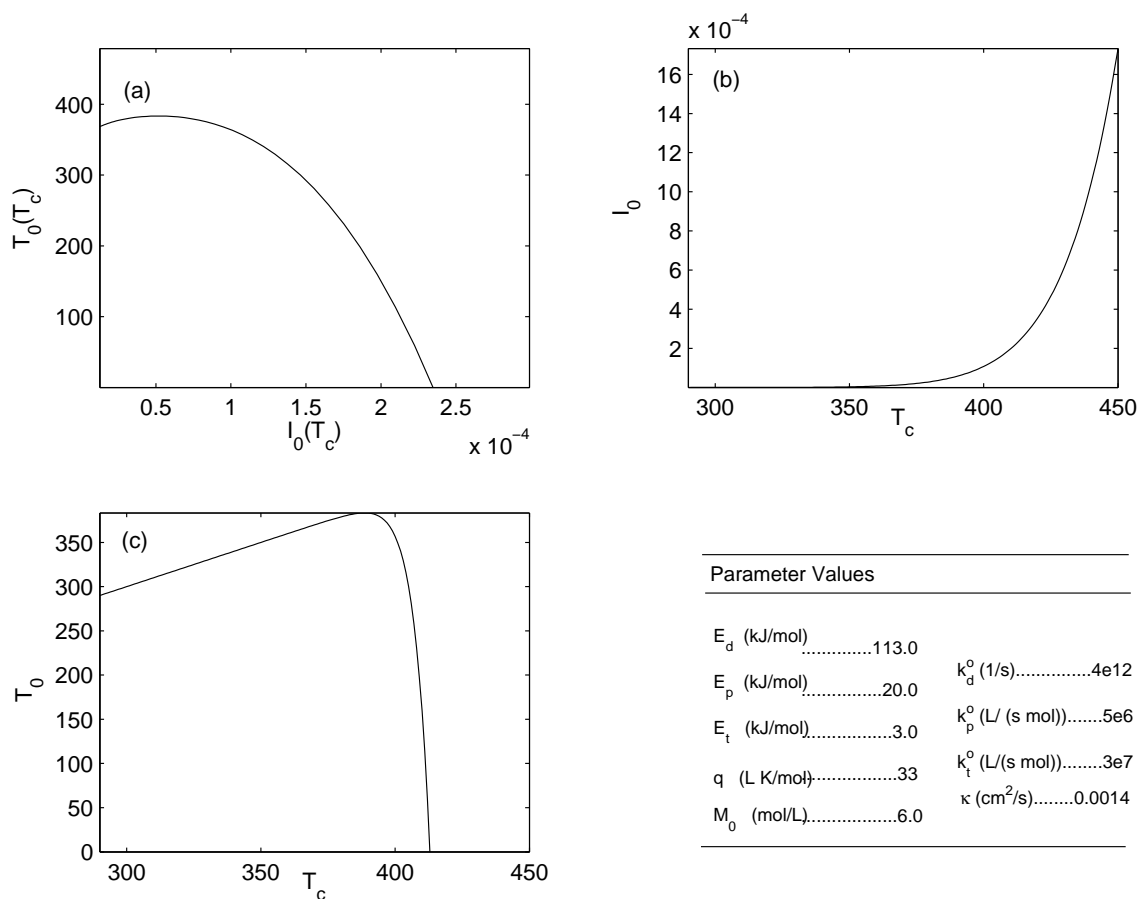
Figure 4.5: Marginal initiation curve for $r = 1.5$ and $\lambda_r^c = 0.66$. Here, A_0 is kept constant and the initial amount of initiator I_0 in mol/L and initial temperature T_0 in degrees K are plotted as functions of the scaling temperature T_c. For values of (I_0, T_0) on and above the curve in (a) initiation will occur. The dimensional parameter values used are given in the accompanying table.
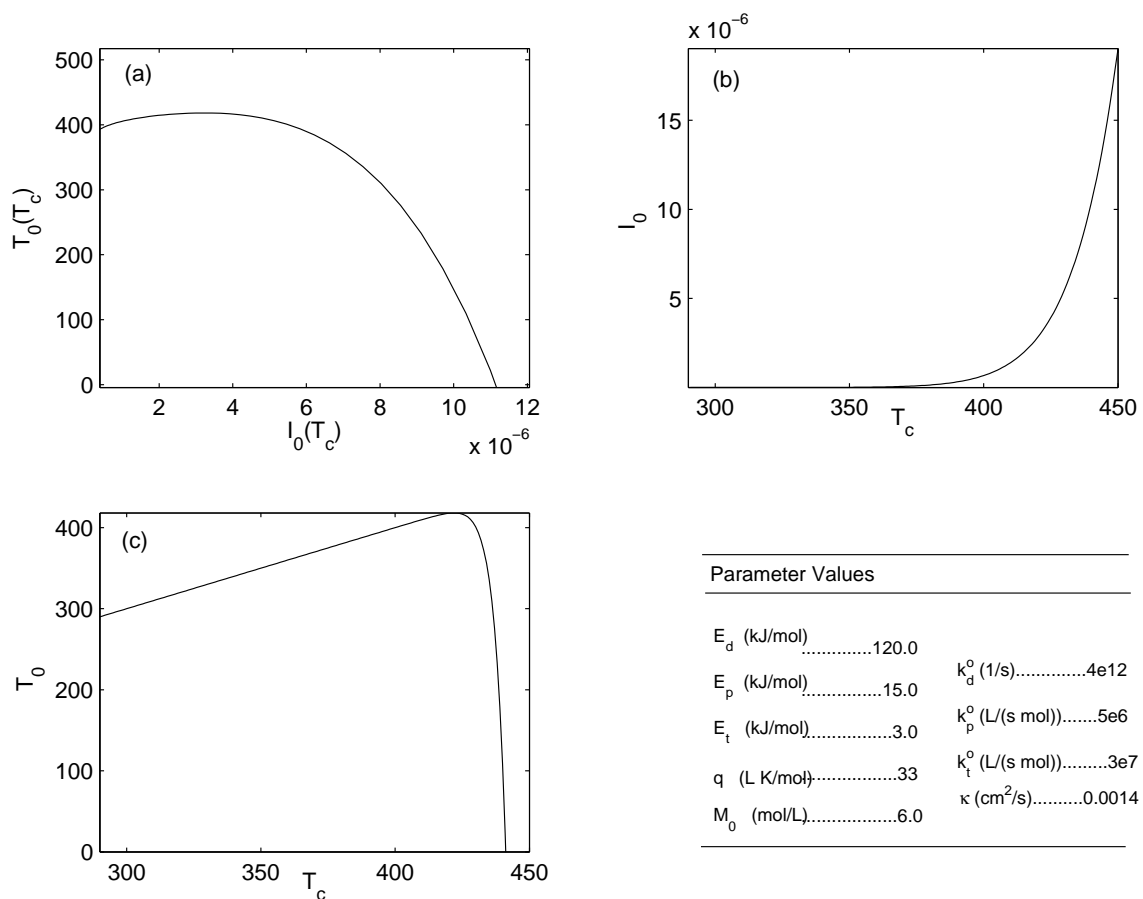
Figure 4.6: Marginal initiation curve for $r = 1.6$ and $\lambda_r^c = 0.54$. Here, A_0 is kept constant and the initial amount of initiator I_0 in mol/L and initial temperature T_0 in degrees K are plotted as functions of the scaling temperature T_c. For values of (I_0, T_0) on and above the curve in (a) initiation will occur. The dimensional parameter values used are given in the accompanying table.

Chapter 5

Additional Systems and Considerations

5.1 Initiation of Polymerization Waves with Newtonian Heat Loss

In this chapter, we will again consider the reduced (dimensional) model for frontal polymerization as given in equations (2.8)–(2.10). However, we will assume that the boundary condition at the end of the tube is that of a prescribed temperature, and we will introduce Newtonian heat loss with heat loss parameter $\hat{\alpha} \geq 0$. The system of equations to be studied is

$$\frac{\partial I}{\partial \hat{t}} = -k_d(T)I, \quad I(0) = I_0 \tag{5.1}$$

46

$$\frac{\partial M}{\partial \hat{t}} = -k_{eff}(T)M\sqrt{I}, \quad M(0) = M_0 \tag{5.2}$$

$$\frac{\partial T}{\partial \hat{t}} = \kappa \frac{\partial^2 T}{\partial \hat{x}^2} + qk_{eff}(T)M\sqrt{I} - \hat{\alpha}(T - T_0), \quad T(0,\hat{x}) = T_0 \quad \hat{x} \geq 0, \tag{5.3}$$

$$T(\hat{t}, 0) = T_w, \quad \text{and} \quad \frac{\partial T}{\partial \hat{x}} \to 0 \quad \text{as} \quad x \to \infty. \tag{5.4}$$

This is derived from the system (2.2)–(2.6) in the same way as equations (2.8)–(2.10). The QSSA and the same simplifying assumptions are used, and the definition of the effective reaction rate is as given in chapter 2. In this analysis, we assume that the temperature at the wall (end of the test tube) T_w is constant.

This system does not lend itself to an asymptotic analysis analogous to the one in chapter 3 because initiation, when it occurs, does not necessarily occur at the wall but rather at some unknown location away from the wall. Instead, we conduct a numerical study of initiation of polymerization waves and the dependence of initiation on the various parameters governing the system's behavior. We begin by introducing a convenient coordinate change to obtain a nondimensional system of equations. We will use the nondimensional parameters

$$r = \frac{E_d}{E_{eff}}, \quad \beta = \frac{R_g T_w}{E_{eff}}, \quad \delta = \frac{R_g T_w^2}{qM_0 E_{eff}},$$

$$t_* = \frac{e^{1/\beta}}{k_{eff}^0}, \quad x_* = \sqrt{\kappa t_*}, \quad \alpha = \hat{\alpha} t_*.$$

We also define the nondimensional variables

$$J = \sqrt{\frac{I}{I_0}}, \quad \Psi = \frac{M_0 - M}{M_0}, \quad \theta = \frac{T - T_w}{\beta T_w},$$

$$\theta_0 = \frac{T_0 - T_w}{\beta T_w}, \quad t = \hat{t}/t_*, \quad \text{and} \quad x = \hat{x}/x_*.$$

Substitution of these variables into equations (5.1)–(5.4) yields the nondimensional equations

$$\frac{\partial J}{\partial t} = -DJ \exp\left(\frac{r\theta}{1+\beta\theta}\right), \quad J(0,x) = 1 \tag{5.5}$$

$$\frac{\partial \Psi}{\partial t} = (1-\Psi)J \exp\left(\frac{\theta}{1+\beta\theta}\right), \quad \Psi(0,x) = 0 \tag{5.6}$$

$$\frac{\partial \theta}{\partial t} = \frac{\partial^2 \theta}{\partial x^2} + \frac{1}{\delta}(1-\Psi)J \exp\left(\frac{\theta}{1+\beta\theta}\right) - \alpha(\theta - \theta_0), \quad \theta(0,x) = \theta_0 \tag{5.7}$$

$$\theta(t,0) = 0 \quad \text{and} \quad \frac{\partial \theta}{\partial x} \to 0 \quad \text{as} \quad x \to \infty \tag{5.8}$$

governing the system. The parameter D appearing in the initiator equation is the analog of the parameter A appearing in equation (2.12) and is defined as

$$D = \frac{k_d(T_w)}{2k_{eff}(T_w)}.$$

As was the case for the parameter A, the magnitude of D indicates the rate at which initiator is consumed during the polymerization process. If D is very large, we would expect that a propagating reaction front would not be observed since the initiator necessary for the reaction to be induced would immediately be depleted. In the current, study we seek an initiation criterion as the relationship between this initiator consumption rate and the amount of heat lost to the environment. The later is inherent in the value of the parameter α. For fixed values of β, r, δ and θ_0 the system (5.5)–(5.8) was solved numerically. The Method of Lines was employed

to obtain a system of ordinary differential equations corresponding to (5.5)–(5.8). In particular, we chose an equally spaced discretization of the spatial variable— $x_i = i\Delta x$ for $i = 0, 1, \ldots, K$—and assumed that each of the variables $J(t, x)$, $\Psi(t, x)$ and $\theta(t, x)$ are well approximated by an interpolation at the points x_i. We let $J_i(t) = J(t, x_i)$, $\Psi_i(t) = \Psi(t, x_i)$ and $\theta_i(t) = \theta(t, x_i)$, and used a central difference approximation formula for the spatial derivative:

$$\left.\frac{\partial^2 \theta}{\partial x^2}\right|_{x=x_i} \approx \frac{\theta_{i+1}(t) - 2\theta_i(t) + \theta_{i-1}}{\Delta x^2} \quad \text{for} \quad i = 1, \ldots, K - 1.$$

At the left most end point, we set

$$\frac{\partial \theta}{\partial t} = 0,$$

and at the imposed right end point we use the approximation

$$\left.\frac{\partial^2 \theta}{\partial x^2}\right|_{x=x_K} \approx \frac{2\theta_{K-1}(t) - 2\theta_K(t)}{\Delta x^2}.$$

The latter follows from the condition that there is zero heat flux in the far field $(\partial/\partial x)\theta(t, x_K) = 0$. Together with equations (5.5)–(5.8), these assumptions define a $3K + 3$ system of ordinary differential equations for the J_i, Ψ_i and θ_i. This system was solved using the LSODA differential equation solver by L. R. Petzold and A. C. Hindmarsh. This package automatically switches between stiff and nonstiff methods of solution at each time step so as to minimize computational time while preserving accuracy. For each numerical computation, the value of $D \in (0, 6)$ was fixed and α was varied until a critical value $\alpha_c(D)$ was found such that for $\alpha < \alpha_c(D)$ a traveling wave solution was observed but for $\alpha > \alpha_c(D)$ either front formation is not observed or the front is seen to be dampened before wave propagation can

begin. Figures 5.1 and 5.2 show these observed phenomena (front formation and propagation or failure of a front to form) for selected values of D. An unambiguous change in the qualitative behavior of the temperature profile is seen as α is varied near the critical value. The curve obtained by the pairs $(D, \alpha_c(D))$ represents a marginal initiation curve for the system. The nature of this curve is also dependent on the values of δ and θ_0.

The adiabatic temperature defined by $T_a = T_0 + qM_0$ is the total increase in temperature due to complete conversion of monomer. Defining the nondimensional adiabatic temperature in the natural way

$$\theta_a = \frac{T_a - T_w}{\beta T_w},$$

we find that the parameter $\delta^{-1} = \theta_a - \theta_0$. Hence δ^{-1} represents the (nondimensional) adiabatic temperature increase attainable during an experiment. For fixed β, θ_0, and M_0 an increase (decrease) in δ^{-1} corresponds to an increase (decrease) in the value of q which we recall is the amount of heat released per unit reacted monomer. Thus, we expect that a decrease in the value of δ would result in a larger portion of the parameter space (D, α) corresponding to the initiation regime. In figure 5.3, the marginal initiation curves for three values of δ are shown. For each value of δ, the region lying below the corresponding curve is the set of (D, α) that will lead to initiation of a polymerization front. As anticipated, this region is increased by taking smaller values of δ. The points that lie above a given curve correspond to the noninitiation regime in which heat lost to the environment (or excessive depletion of initiator) inhibits the formation of a reaction front.

A similar analysis can be made with respect to the initial temperature. For fixed values of β, T_w, δ and M_0 an increase (decrease) in θ_0 corresponds to a proportional

increase (decrease) of the initial temperature in the original, dimensional coordinates. An increase in the initial energy of the system would be expected to result in a larger portion of the parameter space (D, α) corresponding to an initiation regime. That is, for fixed D a reaction front is attainable even with greater heat losses to the surrounding environment. In figure 5.4, this is confirmed. Figure 5.4 shows the marginal initiation curves for three values of θ_0 keeping β and δ fixed. As in figure 5.3, for each curve the regions below and above the curve correspond to the initiation and noninitiation regimes, respectively. Given known (dimensional) values of various kinetic and other parameters (e.g. initial concentrations), it is possible to ensure a reaction wave will form during an experiment by imposing the appropriate temperature at the wall.

5.2   Polymerization by Radially Propagating Front

In this final section, we will examine a phenomenon that has been reported by Asakura *et al.* [1], namely the spontaneous formation of a polymerization front in the center of a cylindrical tube and the ensuing propagation of this front radially outward toward the walls of the tube. Asakura and co-workers intended to produce poly(methyl methacrylate) by immersing a tube of methyl methacrylate and initiator in a thermostatic oil bath. As discussed in this dissertation, polymerization by thermal, free-radical frontal polymerization is typically initiated in a neighborhood of an imposed external heat source as a direct result of contact with this heat source. Hence, they expected to induce a reaction front at the walls of the tube that would propagate into the interior of the mixture. All of their attempts to induce a polymerization front at the walls of the tube using the oil bath as a heat

source failed. They did, however, observe the spontaneous formation of a spherical front at the center of the mixture; this front then propagated radially outward to form the desired polymer. Whether a front formed or not depended on various factors including the temperature of the surrounding bath and the diameter of the test tube. These experimentalists recorded observing a critical tube diameter at which the behavior of the reaction changed. The chemical conversion occurred more "abruptly" in larger test tubes [1]. In this section, we present a mathematical model of the spontaneous front formation described above and offer the results of numerical computations based on this model with special attention given to the effects of bath temperature and tube radius.

We begin by considering a cross section of the test tube taken perpendicular to its length as depicted in figure 5.5. We impose a radial coordinate x as the distance from the center of the test tube $x = 0$ and assume that the behavior of the system is symmetric with respect to the axis $x = 0$. This symmetry assumption implies a no flux boundary condition on the temperature at $x = 0$. The wall of the tube is at $x = \frac{L}{2}$ where L is the diameter of the test tube. Here, the system is in contact with the thermostatic oil bath. Hence, we impose the boundary condition on the temperature θ of the mixture $\theta(t, L/2) = \theta_b$, the bath temperature. Assuming a planar geometry and that spatial variations occur only in the x-direction, the governing equations are the same as (5.5)–(5.7), but the boundary conditions are as just described. The system can be written as

$$\frac{\partial J}{\partial t} = -DJ \exp\left(\frac{r\theta}{1 + \beta\theta}\right), \quad J(0, x) = 1 \tag{5.9}$$

$$\frac{\partial \Psi}{\partial t} \;=\; (1 - \Psi) J \exp\left(\frac{\theta}{1 + \beta\theta}\right), \quad \Psi(0, x) = 0 \tag{5.10}$$

$$\frac{\partial \theta}{\partial t} \;=\; \frac{\partial^2 \theta}{\partial x^2} + \frac{1}{\delta}(1 - \Psi) J \exp\left(\frac{\theta}{1 + \beta\theta}\right), \quad \theta(0, x) = \theta_b \tag{5.11}$$

$$\frac{\partial \theta}{\partial x}(t, 0) \;=\; 0 \quad \text{and} \quad \theta\left(t, \frac{L}{2}\right) = \theta_b. \tag{5.12}$$

For the present problem, the term T_w appearing in the nondimensionalization is a constant scaling temperature; we can take this scaling temperature to be the adiabatic temperature defined in the previous section. Otherwise, the parameters and variables are those defined in section 5.1. Since the system is immersed in a thermostatic bath, we assume that there is no appreciable volumetric heat loss.

The system (5.9)–(5.12) was solved numerically using the LSODA solver package for different values of the bath temperature and the tube radius. Considering a fixed bath temperature, we found that a polymerization front forms (or fails to form) based on the size of the test tube. In figure 5.6, spatial temperature profiles at selected times are shown for a fixed bath temperature and four different choices of the tube diameter. We see that for a (nondimensional) tube radius less that some critical value, a front fails to form. The oil bath is intended as a heat source, but its presence has different effects at various stages of the experiment. This bath, while having a high temperature as compared with normal room temperatures (Asakura *et al.* used bath temperatures of 45^oC to 60^oC), has a temperature that is lower than an expected reaction temperature. During the initial stages of the experiment the temperature in the mixture increases due to contact with the oil bath. A build up of heat in the interior of the mixture eventually acts as a catalyst causing initiator to decompose so that initiation takes place. The temperature increase due to polymer

chain growth (when it occurs) results in a mixture temperature that is much higher than the surrounding bath which at this stage of the experiment serves as a heat sink. Thermally induced frontal polymerization under these experimental conditions thus requires the test tube be sufficiently large so as to decrease the mixture contact with the heat sink. This is evident in figure 5.6. Figure 5.7 shows the spatial profile of the reaction term, $\delta^{-1}\frac{\partial\Psi}{\partial t}$, at selected times for the case when a polymerization front forms in the system. A traveling wave solution is seen.

The numerical computations failed to yield a precise "critical radius" because an intermediate behavior—poorly defined front formation—is observed for values of the radius between those that result in an obvious front and those that clearly result in no front formation whatsoever. Table 5.1 shows lower and upper bounds on such a critical radius for various values of the bath temperature. Figure 5.8 shows the change in behavior of both the spatial temperature and reaction term profiles for radii above and below the range of values as shown in table 5.1.

Table 5.1: Bounds on the Critical Radius Needed for Thermal Front Formation

Bath Temp.	Critical Radius (r_c) Bounds	
θ_b	Lower Bound	Upper Bound
-1	0.30	1.00
-2	0.73	1.00
-3	1.25	2.00
-4	3.50	4.00

We have confirmed through this numerical analysis the finding of Asakura *et al.* It is evident that use of a thermostatic bath as an imposed heat source can induce thermal, radially propagating, frontal polymerization. But, when initiation

does occur, it does not do so in a neighborhood of the heat source but rather in the interior of the mixture after sufficient heat build up. If a front does form, then the temperature of the bath is small relative to the reaction temperature meaning that the bath then acts as a heat sink. For this reason, the test tube used must be sufficiently large in diameter to decrease contact of the mixture with the heat sink and insure front formation and propagation.
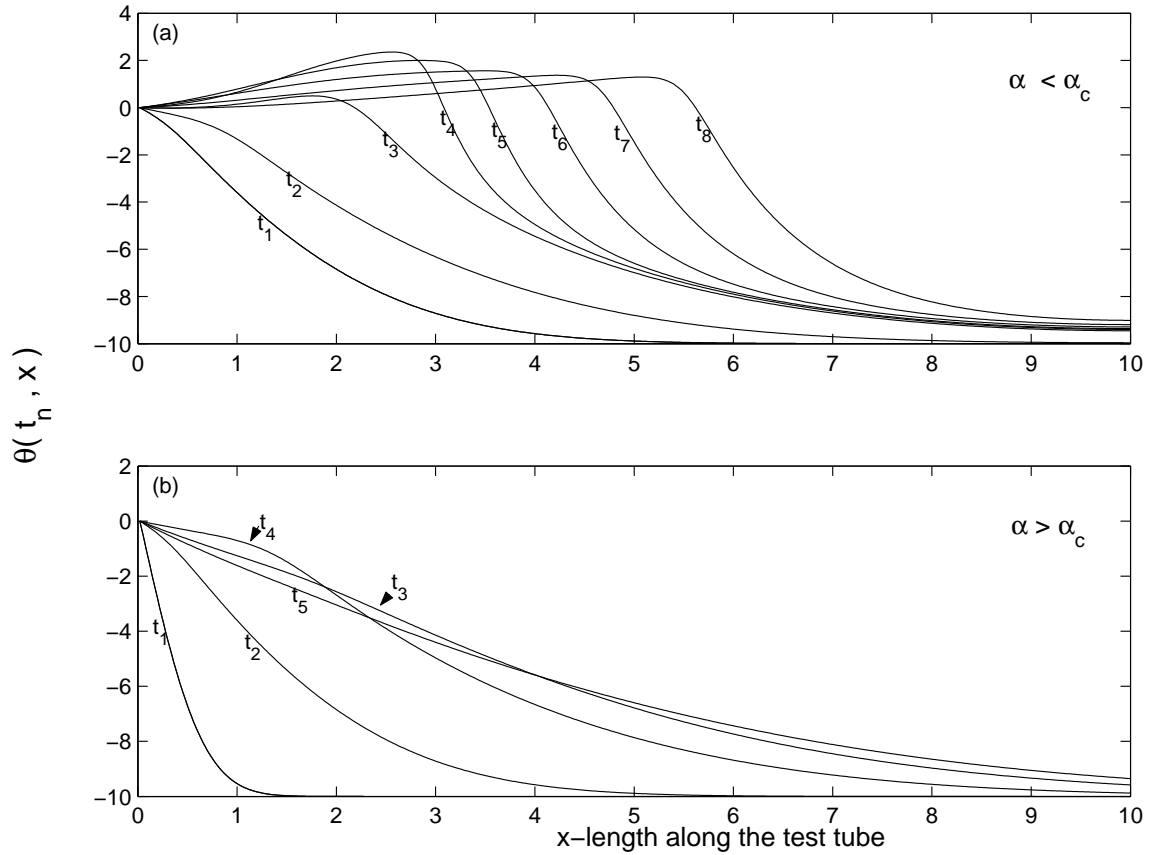
Figure 5.1: Initiation and noninitiation phenomena for $D = 0.5$. In (a), $\alpha = 0.044$ just below the critical value $\alpha_c(0.5) = 0.0443$, and the formation and propagation of a reaction wave is observed. In (b), $\alpha = 0.045$ and a reaction front does not form. The parameter values of $\theta_0 = -10$, $\beta = 0.09$, $\delta = 0.05$, and $r = 2$ were used for both plots. The times for plot (a) are $t_1 = 1.96$, $t_2 = 5.38$, $t_3 = 11.2$, $t_4 = 11.7$, $t_5 = 11.9$, $t_6 = 12.5$, $t_7 = 13.2$, and $t_8 = 14.1$. The times in plot (b) are $t_1 = 0.121$, $t_2 = 1.96$, $t_3 = 8.46$, $t_4 = 13.5$, and $t_5 = 17.1$.
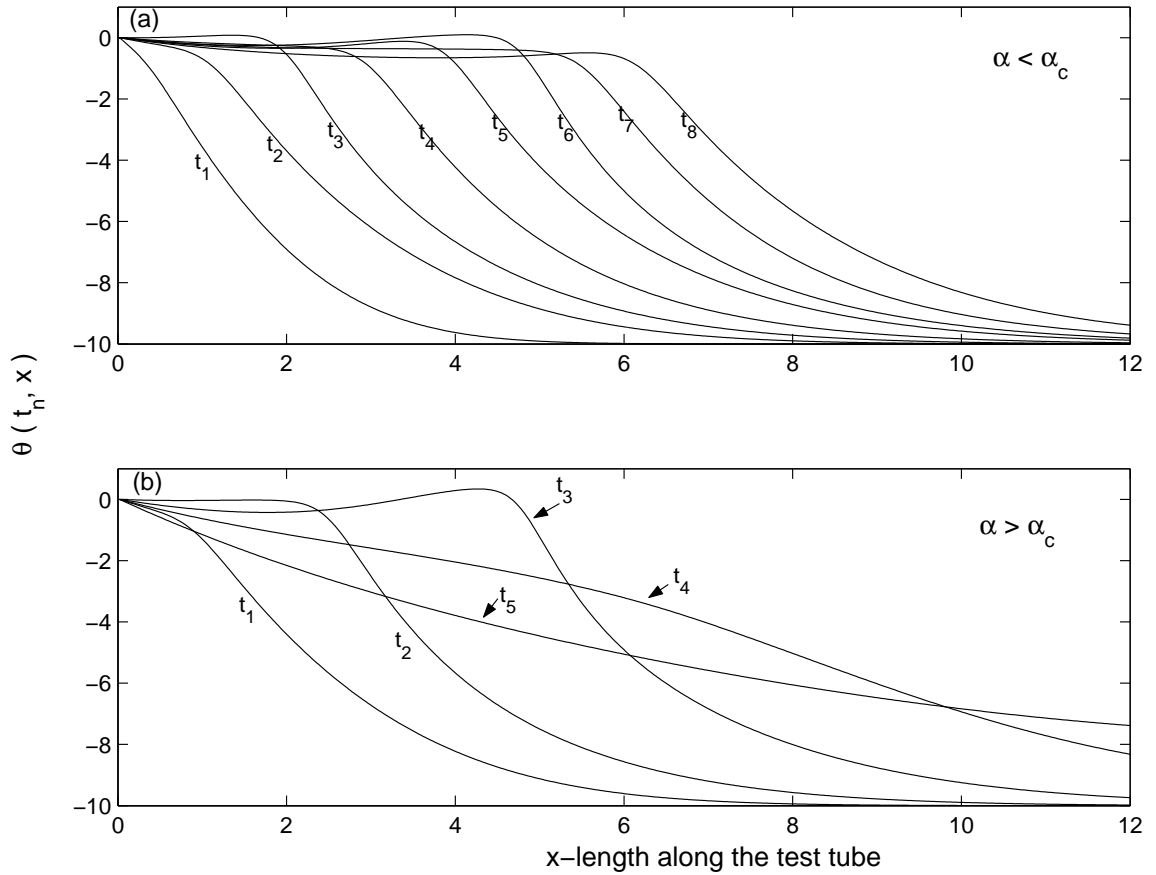
Figure 5.2: Initiation and noninitiation phenomena for $D = 3.0$ with $\alpha < \alpha_c$ (a) and $\alpha > \alpha_c$ (b). The parameter values used in both plots are $\theta_0 = -10$, $\beta = 0.09$, $\delta = 0.04$, $r = 2$, and in (a) $\alpha = 0.017$ and in (b) $\alpha = 0.020$. The critical value is $\alpha_c(3.0) = 0.018$ for the choice of θ_0 and δ. The times at which the temperature profiles are taken are: (a) $t_1 = 1.83$, $t_2 = 4.87$, $t_3 = 6.63$, $t_4 = 8.71$, $t_5 = 11.3$, $t_6 = 12.6$, $t_7 = 14.4$, $t_8 = 16.6$,; (b) $t_1 = 4.23$, $t_2 = 7.73$, $t_3 = 13.8$, $t_4 = 23.2$, $t_5 = 40.1$.

Figure 5.3: Comparison of marginal initiation curves $(D, \alpha_c(D))$ for various values of δ. For each value of δ, the region lying under the corresponding curve represents the pairs (D, α) that lead to initiation of a polymerization wave. Here, $\beta = 0.09$, $\theta_0 = -10$, and $r = 2$.
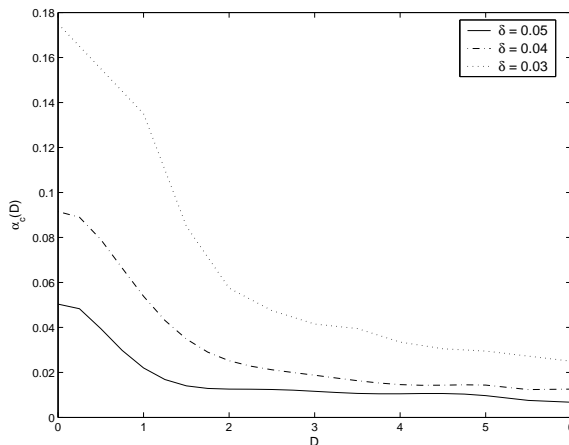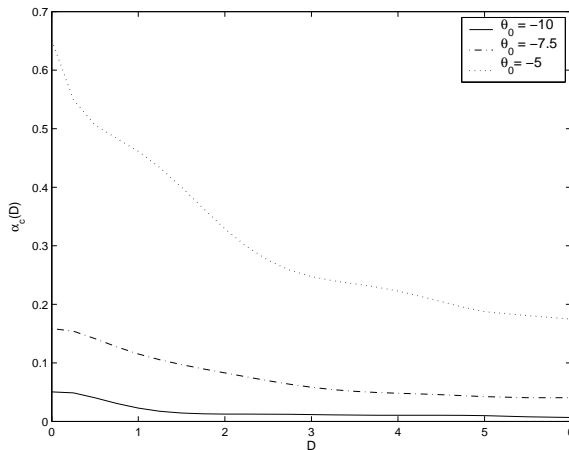

Figure 5.4: Comparison of marginal initiation curves $(D, \alpha_c(D))$ for various values of θ_0. For each value of θ_0 the region lying under the corresponding curve represents the pairs (D, α) that lead to initiation of a polymerization wave. Here, $\beta = 0.09$, $\delta = 0.05$, and $r = 2$.

Figure 5.5: Small section of a test tube showing the imposed coordinate system. Assuming that the behavior of the system, in regards to front formation, is symmetric with respect to $x = 0$, the governing equations are solved on the interval $0 \leq x \leq \frac{L}{2}$ where L is the diameter of the test tube. The temperature is kept at the constant bath temperature at the end $x = \frac{L}{2}$
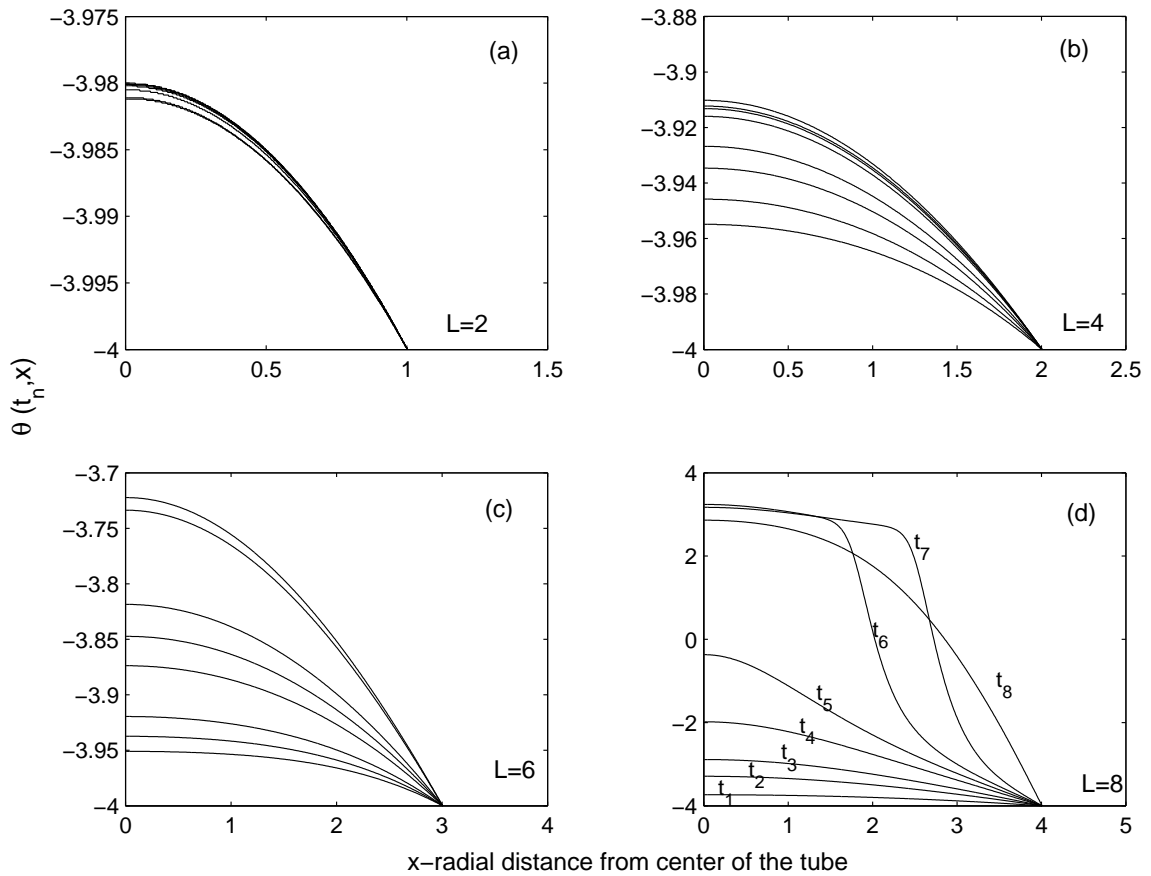
Figure 5.6: Temperature profiles for fixed bath temperature and four different tube radii. The tubes are of diameter (a) L=2, (b) L=4, (c) L=6, and (d) L=8. Only in (d) wh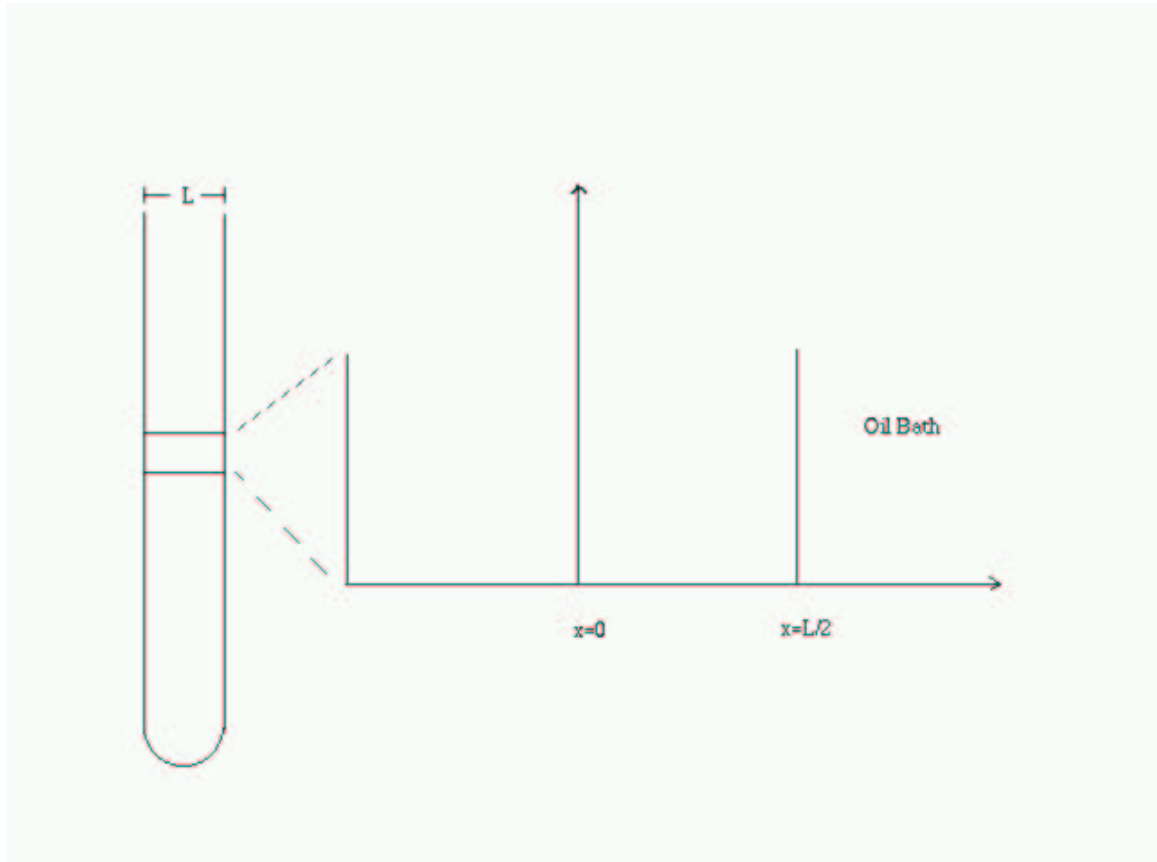ere the diameter of the tube is the largest is there a clear formation and propagation of a reaction wave (note the scaling on the temperature axes). For each of these plots, the parameter values $\theta_b = -4$, $\delta = 0.05$, $\beta = 0.09$ and $r = 2$ were taken. The spatial profiles for (a),(b), and (c) are shown at the approximate times $t = 0.3$, $t = 1.4$, $t = 1.8$, $t = 2$, $t = 3$, $t = 5$, $t = 6$, $t = 15$, and $t = 27$. The profiles in (d) are given at the times $t_1 = 0.03$ $t_2 = 6.49$ $t_3 = 16.4$ $t_4 = 20.7$ $t_5 = 23.3$ $t_6 = 24.4$ $t_7 = 24.6$ and $t_8 = 26.0$.
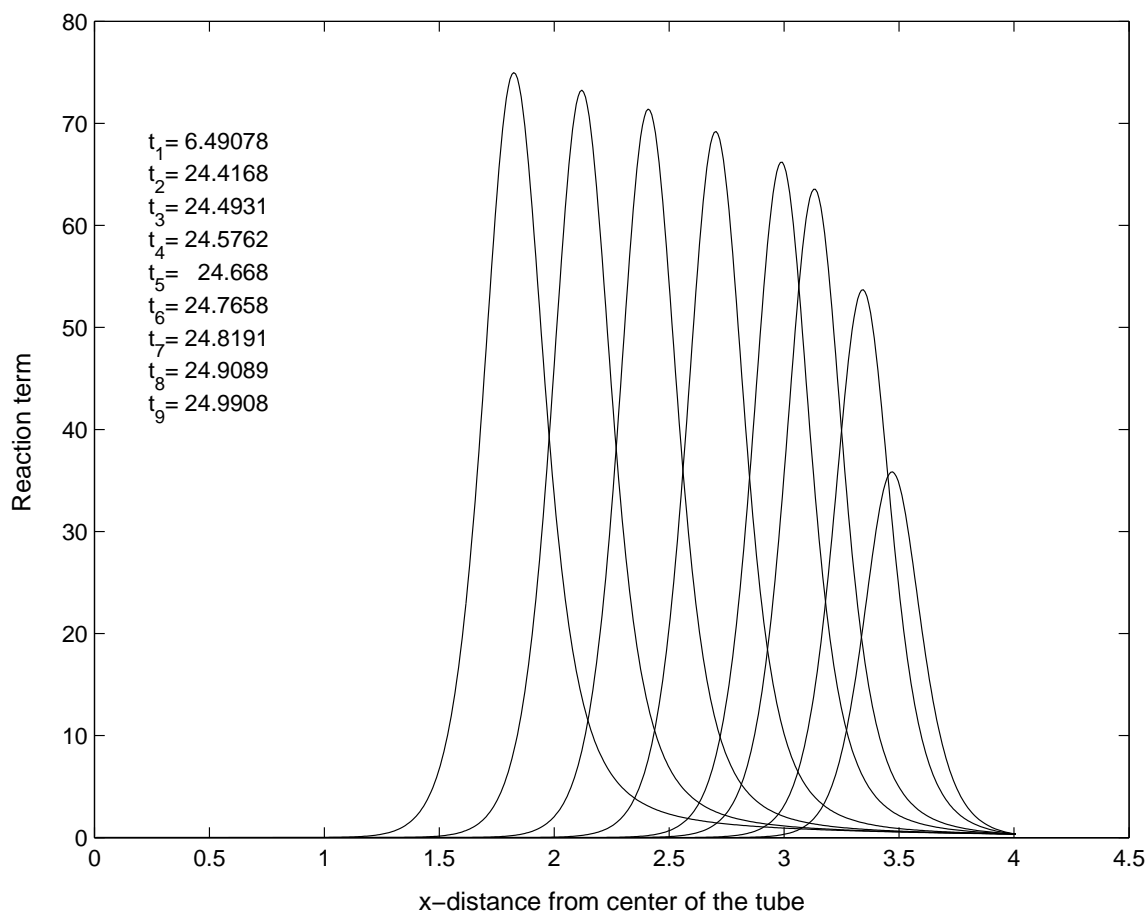
Figure 5.7: Spatial profile of the reaction term $\delta^{-1}\frac{\partial \Psi}{\partial t}$ at several different times. The profiles correspond to the times shown, t_1–t_8 from left to right. The point $x = 4$ marks the wall of the test tube in contact with the oil bath. All parameter values are the same as in figure 5.6 (d). A clear propagating reaction is seen.
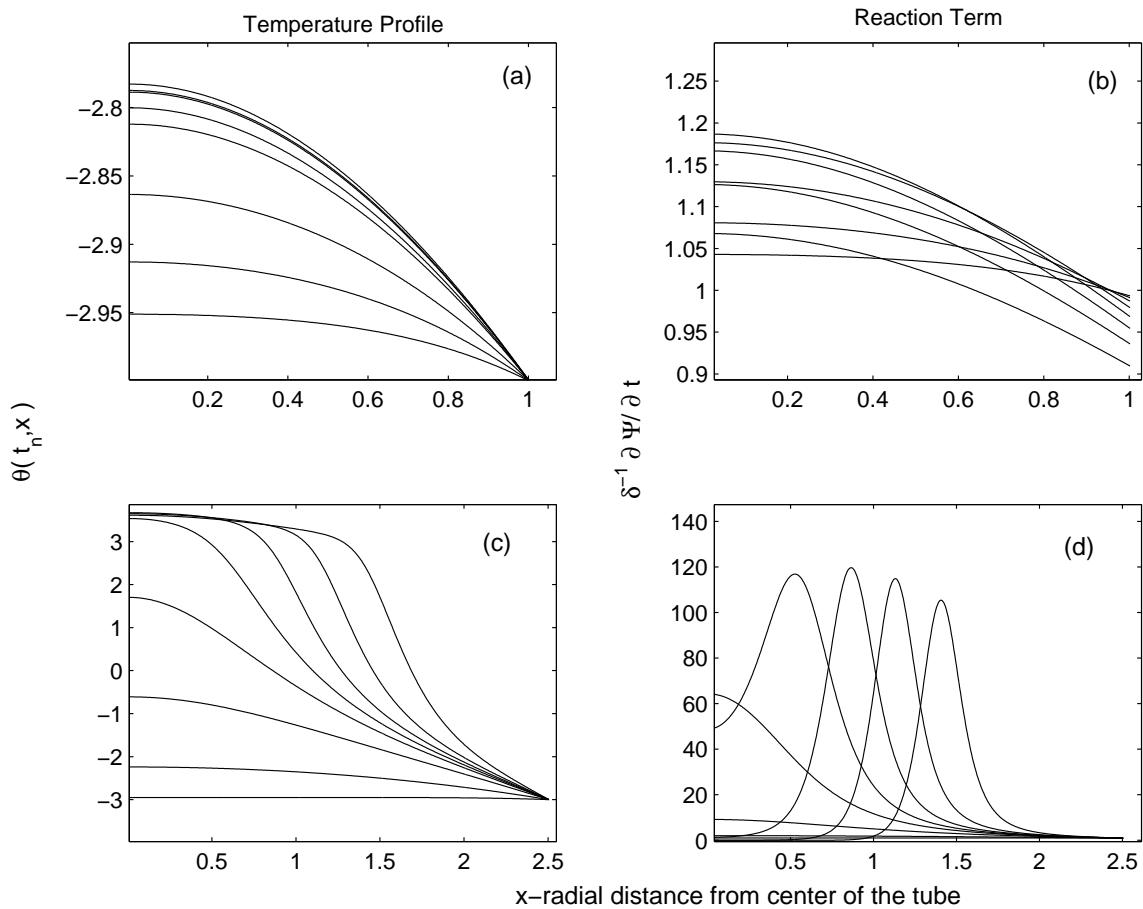
Figure 5.8: Initiation and noninitiation for bath temperature $\theta_b = -3.0$. Figures (a) and (c) show the spatial temperature profiles for several times $0 < t < 6$ for radii below ($L = 1$) and above ($L = 2.5$) respectively the value necessary for front formation. The reaction term profiles for the same radii are shown in (b) and (d). Figure (d) shows an unambiguous traveling wave solution.

Conclusions

One goal of any experiment in free-radical frontal polymerization is to induce the formation of a reaction front that will travel through a mixture of monomer and initiator converting it into a polymer. Only after a reaction front forms can various aspects (front velocity, degree of conversion of monomer, etc.) be examined. Insufficient heat put into the system, inadequate amounts of reactants and heat lost to the environment are some factors that can inhibit reaction front formation. In this dissertation, we have considered thermal frontal polymerization processes given three different types of experimental set ups. Using appropriate mathematical models, we have attempted, for each of these types of experiments, to derive a criterion based on the conditions of the experiment that will allow us to predict when a reaction front will form. This was done by making use of a combination of large activation energy asymptotics and numerical analysis.

We begin by examining a simple experiment in which a mixture of monomer and initiator are placed in a test tube and the temperature is controlled at one end of the tube by a prescribed influx of heat. We used a large activation energy assumption to consider the temperature of the mixture in stages—an inert heating stage where the reaction is negligible leading to a transition stage where heat produced by the reaction starts to become significant. By stretching the time and space coordinates

about the point where the transition heating begins, we are able to locally replace the Arrhenius reaction term with an exponential. This leads to a correction term that is given in terms of a two parameter integral equation. The integral equation exhibits two qualitatively different types of solutions depending on the parameter values. The types of solutions—blow-up solutions and those bounded for all finite time—are interpreted as indicating the formation of a polymerization front or failure of a front to form. The Arrhenius reaction produces a steep temperature gradient at the initiation site (when it occurs) which we associate with blow-up exhibited by the integral equation. By numerically solving the integral equation for a variety of parameter values we were able to obtain an initiation criterion for the system that can be written in terms of the properties of the mixture including kinetic properties (activation energies, frequency factors etc.), initial concentrations of reactants, and the nature of the imposed heat flux. The analysis was carried out in a nondimensional set of coordinates and without restriction to any particular chemical mixture. Hence, the results should be general enough to be considered for any experiment in which the basic set up is as described (one monomer, a prescribed influx of heat, etc.).

Next, we considered an experimental set up similar to the one previously described. But we replaced the heat source with a fixed temperature imposed at one end of the tube, and we added the effect of volumetric heat loss to the environment. A numerical study of this system was performed as we sought an initiation criterion as a relation ship between the parameters governing the state of the mixture. We considered a parameter D that describes the rate of consumption of initiator (the larger the value of D, which is a nonnegative parameter, the faster the initiator is consumed), and a parameter α (also nonnegative) which is determined by the rate

at which heat is lost to the environment. Through a series of numerical computations we were able to determine a critical value $\alpha_c(D)$ such that for each fixed D $\alpha < \alpha_c$ gave rise to front formation and propagation while $\alpha > \alpha_c$ resulted in failure of a front to form. The pairs $(D, \alpha_c(D))$ define a marginal initiation curve for the system. The behavior of this curve was then studied as we varied other parameters governing the system, in particular the initial temperature of the mixture and the adiabatic increase in temperature. We found that increasing the initial temperature or the adiabatic increase in temperature resulted in a larger portion of the parameter space (D, α) corresponding to formation and propagation of a reaction front.

Finally, we examined a phenomenon recently reported by Asakura *et al.* in [1]. Asakura and co-workers attempted to produce reaction waves at the walls of a test tube filled with a monomer and initiator mixture by immersing the tube in a hot, thermostatic oil bath. While they were not successful in inducing reaction at the tube walls, they reported observing the spontaneous formation of a front at the center of the tube. This front then propagated radially outward toward the tube walls. By considering a thin cross-section of the test tube and assuming a planar geometry, we were able to numerically substantiate the experimentalists' observations. We determined that the intended heat source, the oil bath, in fact has two different effects on the system during the various stages of the experiment. Initially, the bath acts as a source of heat since the temperatures used for the bath (45°C to 60°C) are high as compared to normal room temperatures. This allows heat to build up in the mixture. However, this range of bath temperatures is low when compared to a typical reaction temperature. Thus, when a reaction front forms, it does so in the center of the tube farthest from the bath. The role of the oil bath becomes that of a heat sink once a thermal front forms. As was reported by

Asakura *et al.* , we found that front formation depended on the relationship between tube radius and bath temperature. For a fixed bath temperature, a reaction front is more likely to form in larger test tubes. Defining a clear critical radius (as a function of bath temperature) separating initiation and noninitiation conditions is not possible from the model used due to non-thermal mechanisms affecting the mixture. However, lower and upper bounds on tube radius that give rise to a reaction front are presented.

Bibliography

[1] K. Asakura, E. Nihei, H. Harasawa, A. Ikumo, and S. Osanai, *Spontaneous Frontal Polymerization: Propagating front spontaneously generated by locally autoaccelerated free-radical polymerization*, ACS Proceedings (to appear) (2003)

[2] J. Brandrup and E. H. Immergut, *Polymer Handbook*, Wiley, New York, 1989.

[3] N. M. Chechilo, and N. S. Enikolopyan, *Struction of the polymerization wave front and propagation mechanism of the polymerization reaction*, Dokl. Phys. Chem. (1974), 214, pp. 174–176

[4] N. M. Chechilo, and N. S. Enikolopyan, *Effect of the concentration and nature of the initiators on teh propagation process in polymerization*, Dokl. Phys. Chem. (1975), 221, pp. 391–394

[5] N. M. Chechilo, and N. S. Enikolopyan, *Effect of pressure and initial temperature of the reaction mixture during propagation of a polymerization reaction*, Dokl. Phys. Chem. (1976), 230, pp. 840–843

[6] N. M. Chechilo, R. Ya. Khvilivitsky, and N. S. Enikolopyan, *The phenomenon of propagation of the polymerization reaction*, Dokl. Phys. Chem. (1972), 204, pp. 512–513

[7] S. P. Davtyan, P. V. Zhirkov, and S. A. Vol'fson, *Problems of non-isothermal character in polymerization processes*, Russ. Chem. Reviews (1984), 53, pp. 150–163

[8] P. M. Goldfeder, V. A. Volpert, V. M.Ilyashenko, A. M.Khan, J. A. Pojman and S. E. Solovyov, *Mathematical modeling of free-radical polymerization fronts*, J. Phys. Chem. B (1997), 101, pp. 3474–3482.

[9] P. L. Gusika, *The theory of propagation of a polymerization front in a suspension*, Khimicheskaya Fizika, no. 7 (1982) pp. 988–993 (in Russian)

[10] Richard A. Handelsman and W. E. Olmstead, *Asymptotic solution to a class of nonlinear Volterra integral equations*, SIAM J. Appl. Math. Vol. 22, No. 3, (1972), pp. 373–384.

[11] A. K. Kapila, *Evolution and deflagration in a cold combustible subjected to a uniform energy flux*, Internat. J. Engrg. Sci., 19 (1981), pp. 495-509.

[12] Akhtar M. Khan and John A. Pojman, *The use of frontal polymerization in polymer synthesis*, TRIP, Vol. 4, No. 8 (1996), pp. 253–257.

[13] B. B. Khanukaev, M. A. Kozhushner, and N. S. Enikolopyan, *Theory of polymerization front propagation*, Combust. Explos. Shock Waves 10 (1974) pp. 562–569.

[14] B. B. Khanukaev, M. A. Kozhushner, and N. S. Enikolopyan, *Theory of teh propagation of a polymerization front*, Dokl. Phys. Chem. 214 (1974) pp. 84–87.

[15] B. B. Khanukaev, M. A. Kozhushner, N. S. Enikolopyan, and M. N. Chechilo, *Theory of the propagation of a polymerization front*, Combust. Explos. Shock Waves 10 (1974) 17–22.

[16] D. Glenn Lasseigne and W. E. Olmstead, *Ignition of a combustible solid with reactant consumption*, SIAM J. Appl. Math. Vol. 47, No. 2 (1987), pp. 332–342.

[17] A. Liñàn and F. A. Williams, *Theory of ignition of a reactive solid by constant energy flux*, Combustion Sci. Tech., 3 (1971), pp. 91–98.

[18] G. B. Manelis, L. P. Smirnov, and N. I. Peregudov, *Nonisothermal kinetics of polymerization processes. Finite cylindrical reactor.*, Combustion Explosion Shock Waves, 13, (1977), pp. 389–383.

[19] A.G. Merzhanov, *Self-propagating high-temperature synthesis: twenty years of search and findings*, in: *Combustion and Plasma Synthesis of High-Temperature Materials,* (Z.A. Munir, and J.B. Holt, Eds.), VCH, 1990, pp.1-53.

[20] G. Odian, Priniciples of Polymerization 3d ed. New York: John Wiley and Sons (1991)

[21] W. E. OLMSTEAD, *Ignition of a combustible half space*, SIAM J. Appl. Math. Vol. 43, No. 1 (1983), pp. 1–15.

[22] W. E. OLMSTEAD AND RICHARD A. HANDELSMAN, *Asymptotic solution to a class of nonlinear Volterra integral equations II*, SIAM J. Appl. Math. Vol. 30, No. 1, (1976), pp. 180–189.

[23] J. A. POJMAN, *Traveling fronts of methacrylic acid polymerization*, J. Amer. Chem. Soc. 113 (1991) pp. 6284–6286.

[24] J. A. POJMAN, A. M. KHAN, AND W. WEST, *Traveling fronts of adition polymerization: a possible new method of materials synthesis*, Polymer Prepr. Amer. Chem. Soc. Div. Polymer Chem. 33 (1992) pp. 1188–1189.

[25] J. A. POJMAN, I. P. NAGY, AND C. SALTER, *Traveling fronts of addition polymerization with a solid monomer*, J. Amer. Chem. Soc. 115 (1993) pp. 11044–11045.

[26] J. A. POJMAN, J. WILLIS, D. FORTENBERRY, V. ILYASHENKO, AND A. KHAN, *Factors affecting propagating fronts of addition polymerization: velocity, front curvature, temperature profile, conversion and molecular weight distribution*, J. Polymer Sci. Part A: Polymer Chem. 33 (1995) pp. 643–652.

[27] V. S. SAVOSTYANOV, D. A. KRITSKAYA, A. N. PONOMAREV, AND A. D. POMOGAILO, *Thermally initiated frontal polymerization of transition metal nitrate acryamide complexes*, J. Polymer Sci. Part A: Polymer Chem. 32 (1994) pp. 1201–1212.

[28] C. A. SPADE AND V. A. VOLPERT, *On the steady-state approximation in thermal free radical frontal polymerization*, Chemical Engineering Science 55 (2002) pp. 641–654.

[29] V. A. VOLPERT, I. N. MEGRABOVA, S. P. DAVTYAN, AND V. P. BEGISHEV, *Propagation of caprolactam polymerization wave*, Combust. Explos. Shock Waves 21 (1985) pp. 441–447.

Appendix A

Analysis of $I_0(\eta; r, \lambda_r)$ and $I_1(\eta; r, \lambda_r)$

Here, we wish to examine the functions I_0 and I_1 and the asymptotic forms of $\hat{\eta}$ and $\hat{N}$ given in Chapter 4. Recall that I_0 and I_1 were defined as

$$I_0(\eta; r, \lambda_r) = \int_{-\infty}^{\eta} \frac{e^{\sigma}}{\sqrt{\pi(\eta - \sigma)}} F_r\left(\frac{\lambda_r}{r} e^{r\sigma}\right) d\sigma$$

and

$$I_1(\eta; r, \lambda_r) = \lambda_r \int_{-\infty}^{\eta} \frac{e^{(r+1)\sigma}}{\sqrt{\pi(\eta - \sigma)}} \left| F_r'\left(\frac{\lambda_r}{r} e^{r\sigma}\right) \right| d\sigma.$$

First, we see that both of these are monotonically increasing in η by observing that for any $\lambda_r > 0$

$$\frac{\partial}{\partial \eta} I_0(\eta; r, \lambda_r) = \int_{-\infty}^{\eta} \frac{\exp\left(\sigma - \frac{\lambda_r}{r} e^{r\sigma}\right)}{\sqrt{\pi(\eta - \sigma)}} d\sigma > 0 \quad \forall \eta > -\infty,$$

and

$$\frac{\partial}{\partial \eta} I_1(\eta; r, \lambda_r) = \lambda_r \int_{-\infty}^{\eta} \frac{\exp\left((r+1)\sigma - \frac{\lambda_r}{r} e^{r\sigma}\right)}{\sqrt{\pi(\eta - \sigma)}} \, d\sigma > 0 \quad \forall \eta > -\infty.$$

Next, we consider the limit $\lambda_r \to 0$. It is convenient to note the asymptotic expansion of F_r for small values of its argument

$$F_r(x) = 1 - \frac{x}{1+r} + O(x^2) \quad \text{as} \quad x \to 0$$

and the identity

$$\int_{-\infty}^{\eta} \frac{e^{\alpha \sigma}}{\sqrt{\pi(\eta - \sigma)}} \, d\sigma = \frac{e^{\alpha \eta}}{\sqrt{\alpha}}, \quad \text{for all} \quad \alpha > 0.$$

We obtain the asymptotic expansions for I_0 and I_1 as $\lambda_r \to 0$:

$$I_0(\eta; r, \lambda_r) \sim e^{\eta} - \frac{\lambda_r}{r(1+r)^{3/2}} e^{(1+r)\eta} + \dots$$

$$I_1(\eta; r, \lambda_r) \sim \frac{\lambda_r}{(1+r)^{3/2}} e^{(1+r)\eta} - \frac{\lambda_r^2}{r(1+2r)^{3/2}} e^{(1+2r)\eta} + \dots$$

We let $\hat{N}$ and $\hat{\eta}$ be the solution to the system of equations

$$I_0(\hat{\eta}; r, \lambda_r) = \hat{N} e^{-\hat{N}} \tag{A.1}$$

$$I_1(\hat{\eta}; r, \lambda_r) = (\hat{N} - 1) e^{-3\hat{N}}, \tag{A.2}$$

and seek asymptotic expansions for $\hat{N}$ and $\hat{\eta}$ of the form

$$\hat{N} \sim N_0 + \lambda_r N_1 + \dots$$

$$\hat{\eta} \sim \eta_0 + \lambda_r \eta_1 + \dots \quad \text{as} \quad \lambda_r \to 0.$$

Using the expansions of I_0 and I_1 for small λ_r and substituting the assumed expansions of $\hat{N}$ and $\hat{\eta}$ into equations (A.1) and (A.2) we find that

$$N_0 = 1, \quad N_1 = \frac{-1}{(1+r)^{3/2}}$$

$$\eta_0 = -1, \quad \eta_1 = \frac{e^{-r}}{r(1+r)^{3/2}}.$$

To obtain information about the behavior of $\hat{N}$ and $\hat{\eta}$ for large λ_r, we use the identity

$$I_1(\eta; r, \lambda_r) = I_0(\eta; r, \lambda_r) - \int_{-\infty}^{\eta} \frac{e^{\sigma} e^{-\frac{\lambda_r}{r} e^{r\sigma}}}{\sqrt{\pi(\eta - \sigma)}} \, d\sigma.$$

Then, equation (A.1) and (A.2) can be written in the reduced form

$$\int_{-\infty}^{\hat{\eta}} \frac{e^{\sigma} e^{-\frac{\lambda_r}{r} e^{r\sigma}}}{\sqrt{\pi(\hat{\eta} - \sigma)}} \, d\sigma = \hat{N} e^{-\hat{N}} + (\hat{N} - 1) e^{-(1+r)\hat{N}}.$$

Letting N_∞ solve the above as $\lambda_r \to \infty$ and noting that the left hand side of the above goes to zero in this limit, we find that N_∞ is the solution to the transcendental equation

$$N_\infty = (1 - N_\infty) e^{-r N_\infty}.$$

Then from (A.1),

$$N_\infty e^{-N_\infty} = \lim_{\lambda_r \to \infty} \int_{-\infty}^{\hat{\eta}} \frac{e^\sigma}{\sqrt{\pi(\hat{\eta} - \sigma)}} F_r \left(\frac{\lambda_r}{r} e^{r\sigma} \right) d\sigma.$$

To facilitate evaluating the limit on the right, we can use that

$$\int_{-\infty}^{\hat{\eta}} \frac{e^\sigma F_r \left(\frac{\lambda_r}{r} e^{r\sigma} \right)}{\sqrt{\pi(\hat{\eta} - \sigma)}} d\sigma = \int_{-\infty}^{0} \frac{e^\sigma F_r \left(\frac{\lambda_r}{r} e^{r\sigma} \right)}{\sqrt{\pi(\hat{\eta} - \sigma)}} d\sigma + \int_{0}^{\hat{\eta}} \frac{e^\sigma F_r \left(\frac{\lambda_r}{r} e^{r\sigma} \right)}{\sqrt{\pi(\hat{\eta} - \sigma)}} d\sigma.$$

Since F_r is bounded by one, we have

$$\int_{-\infty}^{0} \frac{e^\sigma F_r \left(\frac{\lambda_r}{r} e^{r\sigma} \right)}{\sqrt{\pi(\hat{\eta} - \sigma)}} d\sigma \leq \int_{-\infty}^{0} \frac{e^\sigma}{\sqrt{\pi(\hat{\eta} - \sigma)}} d\sigma = \operatorname{erfc}(\hat{\eta}).$$

Then, making use of the asypmtotic behavior

$$F_r(x) = \frac{\Gamma \left(\frac{1}{r} \right)}{r} x^{-1/r} + O(x^{-1}) \quad \text{as} \quad x \to \infty,$$

we find that as $\lambda_r \to \infty$

$$\int_{-\infty}^{\hat{\eta}} \frac{e^\sigma F_r \left(\frac{\lambda_r}{r} e^{r\sigma} \right)}{\sqrt{\pi(\hat{\eta} - \sigma)}} d\sigma \sim \int_{0}^{\hat{\eta}} \frac{e^\sigma}{\sqrt{\pi(\hat{\eta} - \sigma)}} \frac{\Gamma(\frac{1}{r})}{r} \left(\frac{\lambda_r}{r} e^{r\sigma} \right)^{-1/r} d\sigma + \operatorname{erfc}(\hat{\eta})$$

$$= \frac{2\Gamma(\frac{1}{r})}{\sqrt{\pi} r^{1-1/r}} \sqrt{\frac{\hat{\eta}}{\lambda_r^{2/r}}} + \operatorname{erfc}(\hat{\eta}).$$

Seeking $\hat{\eta}$ in the form

$$\hat{\eta} = \lambda_r^{2/r} \eta_1 + o(\lambda_r^{2/r}) \quad \text{as} \quad \lambda_r \to \infty,$$

we find that

$$\eta_1 = \frac{\pi}{4} r^{2-2/r} \Gamma^2 \left(\frac{1}{r}\right) N_\infty^2 e^{-2N_\infty}.$$

The asymptotic behavior of $\hat{N}$ and $\hat{\eta}$ can be summarized as given in Chapter 4;

$$\hat{N} \quad \sim \quad 1 - \frac{\lambda_r}{(r+1)^{3/2}} + \ldots$$

$$\hat{\eta} \quad \sim \quad -1 + \frac{\lambda_r}{re^r(r+1)^{3/2}} + \ldots \quad \text{as} \quad \lambda_r \to 0$$

and

$$\hat{N} \quad \sim \quad \hat{N}_\infty + \ldots$$

$$\hat{\eta} \quad \sim \quad \lambda_r^{2/r} \left(\frac{\pi}{4\Gamma^2(\frac{1}{r})} r^{2-2/r}\right) \hat{N}_\infty^2 e^{-2\hat{N}_\infty} + \ldots \quad \text{as} \quad \lambda_r \to \infty.$$

Appendix B

Inequalities (4.3) and (4.4)

The mapping T is a contraction on the set of bounded functions S provided N and $\tilde{\eta}$ satisfy the inequalities

$$I_0(\tilde{\eta}; r, \lambda_r) \le N e^{-N} \tag{B.1}$$

and

$$e^N I_0(\tilde{\eta}; r, \lambda_r) + e^{(r+1)N} I_1(\tilde{\eta}; r, \lambda_r) < 1. \tag{B.2}$$

For each fixed value of λ_r, there exists a unique solution $(\hat{N}, \hat{\eta})$ to the corresponding equalities

$$I_0(\tilde{\eta}; r, \lambda_r) = N e^{-N} \tag{B.3}$$

and

$$e^N I_0(\tilde{\eta}; r, \lambda_r) + e^{(r+1)N} I_1(\tilde{\eta}; r, \lambda_r) = 1. \tag{B.4}$$

To demonstrate this, let us consider the case $r = 2$. For this case, we can write

$$I_0(\eta; 2, \lambda_2) \;=\; \sqrt{\frac{\pi}{2\lambda_2}} \int_{-\infty}^{\eta} \frac{\operatorname{erf}\left(\sqrt{\frac{\lambda_2}{2}}e^{\sigma}\right)}{\sqrt{\pi(\eta - \sigma)}} \, d\sigma$$

$$\text{(B.5)}$$

$$I_1(\eta; 2, \lambda_2) \;=\; \sqrt{\frac{\pi}{2\lambda_2}} \int_{-\infty}^{\eta} \frac{\operatorname{erf}\left(\sqrt{\frac{\lambda_2}{2}}e^{\sigma}\right)}{\sqrt{\pi(\eta - \sigma)}} \, d\sigma - \int_{-\infty}^{\eta} \frac{e^{\sigma}e^{-\frac{\lambda_2}{2}e^{2\sigma}}}{\sqrt{\pi(\eta - \sigma)}} \, d\sigma \quad \text{(B.6)}$$

We let $N_1(\eta)$ and $N_2(\eta)$ be defined implicitly by the relations

$$N_1(\eta)e^{-N_1(\eta)} = I_0(\eta; 2, \lambda_2) \tag{B.7}$$

and

$$(N_2(\eta) - 1)e^{-3N_2(\eta)} = I_1(\eta; 2, \lambda_2), \tag{B.8}$$

where the latter equation is obtained by substituting (B.5) into (B.6). An approximate numerical solution of this system was found, and the results are shown in figures B.1 and B.2 for different values of λ_2. The shaded regions are those values of N and η that satisfy the inequalities (4.3) and (4.4).
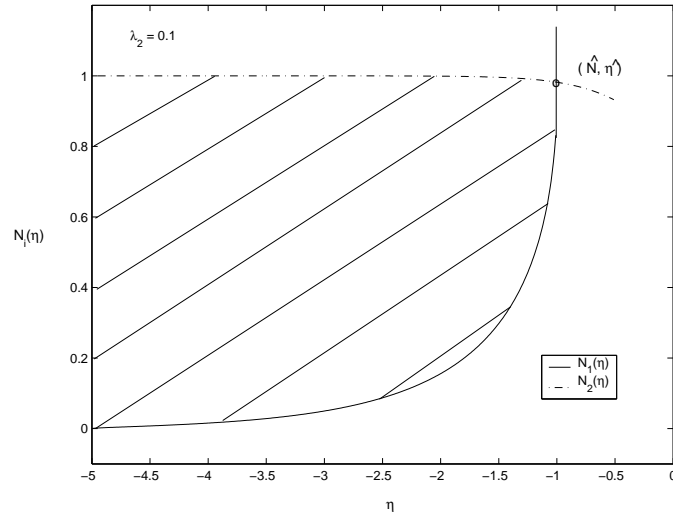
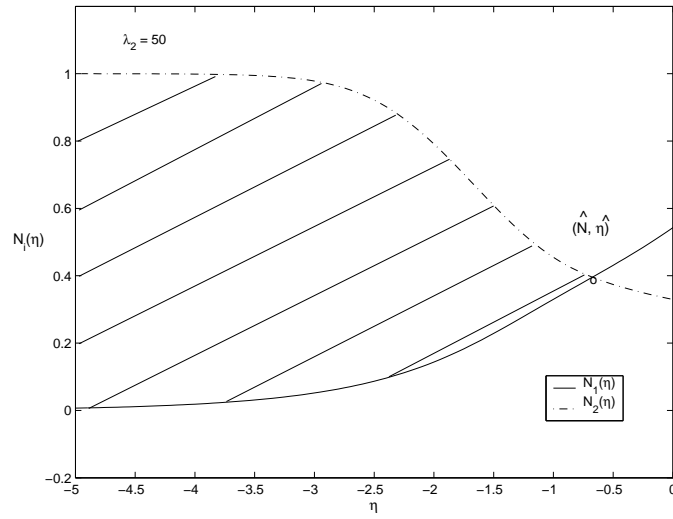Figure B.1: Solution of the system (4.3) and (4.4) for $\lambda_2 = 0.1$

Figure B.2: Solution of the system (4.3) and (4.4) for $\lambda_2 = 50$

Appendix C

Numerical Solution of the Integral Equation

As stated in §4.4, numerical analysis of the integral equation (4.1) first requires that we obtain an approximation to the integral with a finite lower limit of integration. The following expansions for large negative η are given in §4.4.1 and are repeated here for convenience.

$$u \ \sim \ e^{\eta} + \frac{1}{\sqrt{2}}e^{2\eta} + \dots \quad \text{as} \quad \eta \to -\infty \tag{C.1}$$

$$\int_{-\infty}^{\sigma} e^{r(u+s)}\, ds \ \sim \ \frac{1}{r}e^{r\sigma} + \frac{r}{r+1}e^{(r+1)\sigma} + \dots \quad \text{as} \quad \sigma \to -\infty. \tag{C.2}$$

To facilitate the analysis, we can write the integral equation (4.1) as

$$
\begin{aligned}
u(\eta) \ = \ & \int_{-\infty}^{\eta_0} \frac{e^{u(\sigma)+\sigma}}{\sqrt{\pi(\eta-\sigma)}} F_r\left(\lambda_r \int_{-\infty}^{\sigma} e^{r(u(s)+s)}\, ds\right)\, d\sigma \\
& + \int_{\eta_0}^{\eta} \frac{e^{u(\sigma)+\sigma}}{\sqrt{\pi(\eta-\sigma)}} F_r\left(\lambda_r \int_{-\infty}^{\sigma} e^{r(u(s)+s)}\, ds\right)\, d\sigma
\end{aligned}
\tag{C.3}
$$

Assuming η_0 is chosen so that (C.1) and (C.2) hold for η, $\sigma < \eta_0$, the first integral in (C.3) can be evaluated by using the identity

$$\int_{-\infty}^{\eta_0} \frac{e^{\alpha\sigma}}{\sqrt{\pi(\eta-\sigma)}}\, d\sigma = \frac{e^{\alpha\eta}}{\sqrt{\alpha}}\, \mathrm{erfc}\left(\sqrt{\alpha(\eta_0-\eta)}\right)$$

for any $\eta \leq \eta_0$. Similarly, for each $\sigma \geq \eta_0$, the integral in the argument of F_r can be expressed as

$$\int_{-\infty}^{\sigma} e^{r(u(s)+s)}\, ds = \int_{-\infty}^{\eta_0} e^{r(u(s)+s)}\, ds + \int_{\eta_0}^{\sigma} e^{r(u(s)+s)}\, ds$$

$$\sim \frac{1}{r} e^{r\eta_0} + \frac{r}{1+r} e^{(r+1)\eta_0} + \int_{\eta_0}^{\sigma} e^{r(u(s)+s)}\, ds.$$

Combining these results, we arrive at the equation that is to be considered numerically

$$u(\eta) = e^{\eta}\mathrm{erfc}\sqrt{\eta-\eta_0} + \frac{1}{\sqrt{2}} e^{2\eta}\mathrm{erfc}\sqrt{2(\eta-\eta_0)}$$

$$+ \int_{\eta_0}^{\eta} \frac{e^{u+\sigma}}{\sqrt{\pi(\eta-\sigma)}} F_r\left(\lambda_r I_r(\sigma)\right)\, d\sigma,$$

where

$$I_r(\sigma) = \frac{1}{r} e^{r\eta_0} + \frac{r}{r+1} e^{(r+1)\eta_0} + \int_{\eta_0}^{\sigma} e^{r(u(s)+s)}\, ds.$$

The integrand is singular at the upper limit of integration. Hence, we will construct a method based on a product quadrature to avoid any difficulty arising from this singularity.

For each value of $\eta > \eta_0$, we can impose a partition $\eta_0 < \eta_1 < \ldots < \eta_{n+1} = \eta$, and observe that

$$\int_{\eta_0}^{\eta_{n+1}} \frac{e^{u+\sigma}}{\sqrt{\pi(\eta - \sigma)}} F_r\left(\lambda_r I_r(\sigma)\right) \, d\sigma = \sum_{i=0}^{n} \int_{\eta_i}^{\eta_{i+1}} \frac{e^{u+\sigma}}{\sqrt{\pi(\eta_{n+1} - \sigma)}} F_r\left(\lambda_r I_r(\sigma)\right) \, d\sigma.$$

$$(C.4)$$

For ease of notation, we define

$$G(\eta) = e^{\eta + u(\eta)} F_r\left(\lambda_r I_r(\eta)\right).$$

We can then approximate G by a linear Lagrange interpolation. For $\eta \in (\eta_i, \eta_{i+1})$,

$$G(\eta) \approx G(\eta_i) \frac{\eta_{i+1} - \eta}{\Delta \eta_i} + G(\eta_{i+1}) \frac{\eta - \eta_i}{\Delta \eta_i},$$

where $\Delta \eta_i = \eta_{i+1} - \eta_i$. Substituting this approximation into the relation (C.4) gives

$$\int_{\eta_0}^{\eta_{n+1}} \frac{e^{u+\sigma}}{\sqrt{\pi(\eta_{i+1} - \sigma)}} F_r\left(\lambda_r I_r(\sigma)\right) \, d\sigma$$

$$= \sum_{i=0}^{n} \int_{\eta_i}^{\eta_{i+1}} \frac{G(\sigma)}{\sqrt{\pi(\eta_{n+1} - \sigma)}} \, d\sigma$$

$$\approx \sum_{i=1}^{n} \left\{ G(\eta_i) \int_{\eta_i}^{\eta_{i+1}} \frac{\eta_{i+1} - \sigma}{\Delta \eta_i \sqrt{\pi(\eta_{n+1} - \sigma)}} \, d\sigma + G(\eta_{i+1}) \int_{\eta_i}^{\eta_{i+1}} \frac{\sigma - \eta_i}{\Delta \eta_i \sqrt{\pi(\eta_{n+1} - \sigma)}} \, d\sigma \right\}$$

$$= \sum_{i=0}^{n+1} W_{n+1,i}\, G(\eta_i).$$

The quadrature weights $W_{i,j}$ are determined as

$$W_{n+1,i} = \int_{\eta_i}^{\eta_{i+1}} \frac{\eta_{i+1} - \sigma}{\Delta\eta_i \sqrt{\pi(\eta_{n+1} - \sigma)}}\, d\sigma + \int_{\eta_{i-1}}^{\eta_i} \frac{\sigma - \eta_{i-1}}{\Delta\eta_{i-1} \sqrt{\pi(\eta_{n+1} - \sigma)}}\, d\sigma,$$

$$\text{for} \quad i = 1, \ldots, n$$

$$W_{n+1,0} = \int_{\eta_0}^{\eta_1} \frac{\eta_1 - \sigma}{\Delta\eta_0 \sqrt{\pi(\eta_{n+1} - \sigma)}}\, d\sigma$$

$$W_{n+1,n+1} = \int_{\eta_n}^{\eta_{n+1}} \frac{\sigma - \eta_n}{\Delta\eta_n \sqrt{\pi(\eta_{n+1} - \sigma)}}\, d\sigma$$

Letting u_k denote the solution at the time η_k and making use of the above, we use the following implicit scheme to compute the solution of (4.1)

$$u_{n+1} = e^{\eta_{n+1}}\operatorname{erfc}\sqrt{\eta_{n+1} - \eta_0} + \frac{1}{\sqrt{2}}e^{2\eta_{n+1}}\operatorname{erfc}\sqrt{2(\eta_{n+1} - \eta_0)} + \sum_{i=0}^{n+1} W_{n+1,i}\, G(\eta_i)$$

for $n = 0, 1, \ldots$ with u_0 given by (C.1). At each step, the integral appearing in the argument of F_r is computed by the trapezoid rule.

The value of $\eta_0 = -10$ was chosen for all numerical results presented here. The described scheme was implemented for fixed r and λ_r, and in the case of initiation solutions was run until such time as no solution existed to the algebraic equation for u_{n+1}. The blow-up time in these instances was determined by successively refining the computational mesh. The accuracy of the critical values of λ_r and the blow-up times was checked by comparison to the results determined for the case $r = 1$ with those found by Lasseigne and Olmstead in [16].